NBS REPORT

6043

THE USE OF MEASUREMENTS IN PREDICTING THE PERFORMANCE OF TROPOSPHERIC COMMUNICATION CIRCUITS

by

A. P. Barsis, P. L. Rice and K. A. Norton

NBS

U. S. DEPARTMENT OF COMMERCE
NATIONAL BUREAU OF STANDARDS
BOULDER LABORATORIES
Boulder, Colorado

THE NATIONAL BUREAU OF STANDARDS

Functions and Activities

The functions of the National Bureau of Standards are set forth in the Act of Congress, March 3, 1901, as amended by Congress in Public Law 619, 1950. These include the development and maintenance of the national standards of measurement and the provision of means and methods for making measurements consistent with these standards: the determination of physical constants and properties of materials; the development of methods and instruments for testing materials, devices, and structures; advisory services to Government Agencies on scientific and technical problems; invention and development of devices to serve special needs of the Government; and the development of standard practices, codes and specifications. The work includes basic and applied research, development, engineering, instrumentation, testing, evaluation, calibration services, and various consultation and information services. A major portion of the Bureau's work is performed for other Government Agencies, particularly the Department of Defense and the Atomic Energy Commission. The scope of activities is suggested by the listing of divisions and sections on the inside back cover.

Reports and Publications

The results of the Bureau's work take the form of either actual equipment and devices or published papers and reports. Reports are issued to the sponsoring agency of a particular project or program. Published papers appear either in the Bureau's own series of publications or in the journals of professional and scientific societies. The Bureau itself publishes three monthly periodicals, available from the Government Printing Office: The Journal of Research, which presents complete papers reporting technical investigations; the Technical News Bulletin, which presents summary and preliminary reports on work in progress; and Basic Radio Propagation Predictions, which provides data for determining the best frequencies to use for radio communications throughout the world. There are also five series of nonperiodical publications: The Applied Mathematics Series, Circulars, Handbooks, Building Materials and Structures Reports, and Miscellaneous Publications.

NATIONAL BUREAU OF STANDARDS REPORT

NBS PROJECT		NBS REPORT
8370-40-8878	February 24, 1959	6043

THE USE OF MEASUREMENTS IN PREDICTING THE PERFORMANCE OF TROPOSPHERIC COMMUNICATION CIRCUITS

by

A. P. Barsis, P. L. Rice and K. A. Norton

The studies contained in this report are sponsored by Det. 1, Ground Electronics Engineering Installation Agency (STRATCOM)(AMC), United States Air Force.

U. S. DEPARTMENT OF COMMERCE
NATIONAL BUREAU OF STANDARDS
BOULDER LABORATORIES
Boulder, Colorado

TABLE OF CONTENTS

THE USE OF MEASUREMENTS IN PREDICTING THE PERFORMANCE OF TROPOSPHERIC COMMUNICATION CIRCUITS

by

A. P. Barsis, P. L. Rice and K. A. Norton

Summary

The uncertainty in predicting the performance of tropospheric communication circuits may be expressed by a variance, assuming a log-normal distribution of the differences between calculated and measured values of field strength or basic transmission loss, if a number of paths with identical geometrical and other prediction parameters are considered.

It is shown to what extent this variance may be reduced by taking into account transmission loss measurements over the same path for which the prediction is intended, or over a similar path. The "improved prediction" is obtained by assigning weights to calculated and observed values, respectively, and forming a weighted average. The method is demonstrated by examples, and the results are used to calculate new values of service probability on the basis of the improved prediction.

Comparison of service probabilities for predictions based on the calculation above, and for predictions taking into account the results of transmission loss measurements, enables the designer to judge whether the cost of a measurement program is justified in terms of possible savings in equipment for a final installation.

1. Introduction

In a recent report by the authors[1/] a method was given to predict the performance of a tropospheric communication system by the use of semi-empirical methods, and to evaluate the probability of its success by the introduction of the concept of service probability. Briefly, service probability has been defined as the probability of obtaining a specified grade of service or better during a given percentage of the hours in a specified period of time, usually taken to be all hours of the year. The service probability is designated as F(t), and the percentage of the hours during the period considered is termed time availability and designated by p. The specified grade of service is predetermined in terms of an hourly median r.m.s. carrier to r.m.s. noise ratio which takes into account short-term signal fading and the modulation capabilities of the circuit. All three concepts, namely, grade of service, time availability, and service probability are brought together in a single graphical representation. The final graph has two

1/ A. P. Barsis, K. A. Norton, and P. L. Rice, "Predicting the performance of long distance communication circuits," NBS Report 6032, December 1958

probability scales with the ordinate showing the time availability p in percent of all hours and the abscissa showing the service probability F(t). Each curve on the graph corresponds to a system with fixed operating characteristics such as transmitter power, antenna size, etc., and may therefore be labelled by a figure representing installation and operating costs. Various systems may thus be compared on the basis of cost versus service probability. In other words, the cost of various systems may be compared using the probability of success for each system as a yardstick.

From a study of the methods given in Ref. 1 and from an inspection of service probability displays, it is shown that there is an allowance made for uncertainties in the prediction process. This uncertainty is expressed in terms of a normal distribution with standard deviation $\sigma_{rc}(p)$. The standard deviation, $\sigma_{rc}(p)$, includes a term $\sigma_c(p)$ for errors in the estimate of transmission loss, as well as a term σ_r which allows for variations in equipment performance. Fig. 1 shows these uncertainties as derived in Ref. 1. If $\sigma_{rc}(p)$ can be reduced below the values given, then the estimate of the power required for high service probabilities, such as $F(t) = 0.95$, will be reduced accordingly. Also, service probability curves determined by these methods will be less steep, and the expected value p for $F(t) = 0.5$ would constitute a much better estimate since it would not differ as much from the esti-

mates for higher and lower values of service probability. The question is how much the standard deviation $\sigma_{rc}(p)$ can be decreased by taking into account the results of transmission loss measurements made for various periods of time. The uncertainty in the assumption of median r.m.s. carrier to median r.m.s. noise ratio R and of the effective noise figure F, which has been expressed by the standard deviation σ_r, will not be affected by the availability of transmission loss or field strength measurements, and only the $\sigma_c(p)$ portion of the standard deviation $\sigma_{rc}(p)$ can be reduced. $\sigma_c(p)$ as a function of p is shown by curves (a) and (c) on Fig. 1, together with the corresponding weights. The use of the weights will be discussed later.

2. Statistical Basis for Prediction Improvement

Analogous to the prediction uncertainty $\sigma_c(p)$ which was assigned to calculated values of field strength, a standard deviation $\sigma_{oe}(p)$ is assigned to observed field strength values. An improved prediction is then obtained by computing weighted averages of predicted and measured values. In conformance with statistical practice, weights are defined as the reciprocals of the variances. The variance $\sigma_c^2(p)$ has already been defined; $\sigma_c(p)$ and the reciprocal of $\sigma_c^2(p)$ which is the weight $w_c(p)$ are shown on Fig. 1. An expression for $\sigma_{oe}^2(p)$ will be derived in the next section. Most of the terms and symbols used are tabulated in Appendix I.

The general problem considered here is the improvement of predictions made for a specific tropospheric propagation path, using measurements obtained over the same or a slightly different path. It will often be the case that measurements are made only during several weeks or months, while the improved prediction should be applicable to all hours of the year.

As the calculations for tropospheric communication systems are usually in terms of basic transmission loss L_b, the method of prediction improvement will also be treated in these terms. It should be remembered, however, that the two quantities, field strength and basic transmission loss, are directly related, and an hourly median value of field strength E(p) exceeded during at least p% of all hours is equivalent to a basic transmission loss value $L_b(p)$ not exceeded during at least p% of all hours. In the following discussion, all L values are hourly medians, and the p-dependence is implied, although the symbol (p) will be dropped for convenience.

If an observed transmission loss value L_{oa} and a calculated value L_{ca}, both in decibels, are available for Path a, the improved prediction L_{ta} is given by:

$$L_{ta} = \frac{w_{oa} L_{oa} + w_{ca} L_{ca}}{w_{oa} + w_{ca}} \qquad (1)$$

where w_{oa} and w_{ca} are weights assigned to the observed and calculated

values for Path a.

Suppose, however, that an improved prediction L_{tb} is desired for Path b, for which measured values are not available. Calculated values L_{ca} and L_{cb} are available for both paths, and we may estimate L_{tb} as follows:

$$L_{tb} = L_{ta} + (L_{cb} - L_{ca}) \tag{2}$$

The measured value L_{oa} is the sum of a "true value" L_a (independent of p) and a component δ_a of the measurement error associated with the fact that the measurements are made over a finite period of time.*

$$L_{oa} = L_a + \delta_a \tag{3}$$

The computed values, L_{ca} and L_{cb} are the sum of true values L_a and L_b and prediction errors ϵ_a and ϵ_b:

$$L_{ca} = L_a + \epsilon_a, \qquad L_{cb} = L_b + \epsilon_b \tag{4}$$

The expected values of δ_a, ϵ_a and ϵ_b are zero, the expected variance of L_{ca} is $\sigma_{ca}^2 = 1/w_{ca}$, the expected variance of L_{cb} is σ_{cb}^2,

* In addition to this measurement error there will always be some uncertainty in the accuracy of the measurements due to calibration errors; this latter uncertainty is taken to have a variance σ_e^2 and will be introduced later.

and the expected variance of L_{oa} is $\sigma_{oa}^2 = 1/w_{oa}$.

It will be assumed that the correlation between L_{oa} and either L_{ca} or L_{cb} is zero. The correlation between L_{ca} and L_{cb} will be denoted by ρ_{ab}. As a practical matter, it will sometimes be convenient to set ρ_{ab} equal to either zero or one, depending on whether the paths are very different or almost alike.

With the above assumptions, the variance about the estimate of L_{tb} in (2) may be obtained. It is shown in Appendix II that the correlation between L_{ta} and L_{ca} is σ_{ta}/σ_{ca}, where $\sigma_{ta}^2 = 1/(w_{oa} + w_{ca})$ is the variance of the estimate L_{ta}. This is the estimate used when measurements are made over the path for which predictions are desired, and the remaining sections of this paper will be devoted to a derivation of σ_{ta}^2. The correlation between L_{ta} and L_{cb} is $(\sigma_{ta}/\sigma_{ca})\rho_{ab}$. Then the variance associated with the improved prediction (2) for Path b is given by

$$\sigma_{tb}^2 = \sigma_{cb}^2 + \sigma_{ca}^2 - \sigma_{ta}^2 - 2\sigma_{ca}\sigma_{cb}\rho_{ab}(1 - \sigma_{ta}^2/\sigma_{ca}^2) \qquad (5)$$

The detailed derivation of (5) is given in Appendix II.

If Path a is the same as Path b, then $L_{tb} = L_{ta}$, the variances σ_{ca}^2 and σ_{cb}^2 are equal, and $\rho_{ab} = 1$; in this case, (5) reduces to $\sigma_{tb}^2 = \sigma_{ta}^2$ as it should.

It is shown in Appendix II that the correlation coefficient ρ_{ab}

between estimates L_{ca} and L_{cb} over the two Paths a and b has to be at least 0.5 in order to reduce the standard error of estimating L_{tb} below the standard error of L_{cb}. In general, it will be quite difficult to make an accurate estimate of the correlation coefficient ρ_{ab}. The results of the study in Appendix II show that ρ_{ab} has to be very close to unity in order to obtain a substantial improvement in the estimate of L_{tb} over the estimate L_{cb} obtained without any measurements. Available data which may be used to estimate ρ_{ab} are contained in papers by Kirby and Capps[2], and Kirby[3]. It is shown there that for a fixed transmitter location the serial correlation coefficient between field strength values observed at adjacent measuring locations drops to 0.5 within a distance of one-half to one mile. On the other hand, Kirby, et al[4], have shown that there is relatively high correlation between different frequencies received over essentially the same paths. All these results were obtained on much shorter paths than are normally used for tropospheric scatter communication systems, and may not be directly applicable. To the extent that these measurements are applicable it would appear that path loss measurements made on paths with one or the other of their terminals separated by as much as one mile from the

2/ R. S. Kirby and F. M. Capps, "Correlation in VHF propagation over irregular terrain," IRE Trans. PGAP, Vol. AP-4, No. 1, pp. 77-85, January 1956

3/ R. S. Kirby, "Measurement of service area for television broadcasting," IRE Trans. PGBTS-7, pp. 23-30, February 1957

4/ R. S. Kirby, H. T. Dougherty, and P. L. McQuate, "VHF propagation measurements in the Rocky Mountain region," IRE Trans. PGVC-6, pp. 13-19, July 1956 (see Fig. 6)

terminals of the path for which a prediction is required will be of little or no direct value.

The method of obtaining the variance $\sigma_{oe}^2(p)$ and weight $w_o(p)$ for a set of measurements and the procedure for applying them to all day-all year estimates will be discussed in the following section.

3. Estimating the Standard Deviation $\sigma_{oe}(p)$

The variance $\sigma_{oe}^2(p)$ associated with an observed field strength value $E_o(p)$, or the equivalent basic transmission loss $L_{bo}(p)$ may be separated conveniently into two parts $\sigma_o^2(p)$, and σ_e^2, so that

$$\sigma_{oe}^2(p) = \sigma_o^2(p) + \sigma_e^2 \qquad (6)$$

In this representation σ_e is the "equipment," or reading error, taken to be independent of the percentage of hours, p. The part $\sigma_o(p)$, however, is considered to be a function of the time availability p in percent of hours, the number of days of measurement, n, and the angular path distance, θ. Thus $\sigma_o^2(p)$ is that part of the variance of observed values $L_{bo}(p)$ independent of the error σ_e introduced by the measuring equipment and procedures.

The weight $w_o = 1/\sigma_o^2(p)$ associated with measurements extending over a short period of time is less than the weight associated with the median of basic transmission loss values observed over a long period. If only one hourly median were available for some path, for instance, it would be the only available estimate of $L_{bo}(50)$. The variance

$\sigma_o^2(p = 50\%, N = 1 \text{ hour})$ associated with one hourly median is simply the variance of all hourly medians that might have been recorded over the path.

Analysis of a large amount of tropospheric propagation data has resulted in the determination of the dependence of $\sigma_o^2(50)$ on the number of days of observation. There is so much more correlation between measurements made during successive hours of one day than there is between measurements made at the same hour on successive days, that the total number of days is a better measure of sample size than the total number of hours. One might conclude then that one hour of observation a day for a great many days is worth almost as much as a continuous period of recording. However, an exception to the above statement needs to be made in order to take care of the commonly observed diurnal variation of radio transmission loss. As in earlier work[1, 5, 6/], the hours of the year are grouped into "time blocks" which divide the day into four parts and the year into two parts, winter and summer. An examination of the dependence of $\sigma_o^2(50)$ on the number

5/ P. L. Rice, A. G. Longley, and K. A. Norton, "Prediction of the cumulative distribution with time of ground wave and tropospheric wave transmission loss," NBS Report 5582, June 1958

6/ K. A. Norton, P. L. Rice, L. E. Vogler, "The use of angular distance in estimating transmission loss and fading range for propagation through a turbulent atmosphere over irregular terrain," Proc. IRE, 43, No. 10, pp. 1488 - 1526, October 1955

of days, n, was then made for each time block. Table I below lists all time blocks.

Table I

Time Blocks

No.	Month	Hours
1	November-April	0600-1300
2	November-April	1300-1800
3	November-April	1800-2400
4	May-October	0600-1300
5	May-October	1300-1800
6	May-October	1800-2400
7	May-October	0000-0600
8	November-April	0000-0600

It has also been found convenient to combine the four time blocks pertaining to the winter season (1, 2, 3 and 8) and designate this combination as a time block group. Similarly, the combined Time Blocks 4, 5, 6 and 7 form another time block group pertaining to the summer season. From the analysis of a large amount of propagation data more fully described in Ref. 6, an empirical relation has been determined between the hourly median value of field strength (or basic transmission loss) calculated for Time Block 2 (the average winter afternoon hour) and the hourly median applicable to any desired percentage of hours within a specific time block or time block group.

This relation is given by the $V(p, \theta)$ curves shown on Figs. 2,

3 and 4, where the hourly median basic transmission loss $L_{bm}(p)$ corresponding to the field strength value exceeded during p% of all hours is given by

$$L_{bm}(p) = L_{bm}(50) - V(p, \theta) \qquad (7)$$

In (7), $L_{bm}(50)$ is <u>always</u> the Time Block 2 median value (calculated in accordance with the methods given in Ref. 5), and the value $V(p, \theta)$ is read from Figs. 2, 3 or 4, depending on whether the distribution of hourly medians is desired for the winter time block group (later designated by "F"), the summer time block group (similarly designated by "S"), or for all hours of the year (designated by "A").

Graphs similar to Figs. 2, 3 and 4, but for individual time blocks are contained in Ref. 5.

From an analysis of long-term data from 12 propagation paths having a mean angular distance of θ = 18.2 milliradians, a variance curve of $\sigma_{oo}^2(50)$ versus n for θ = 18.2 milliradians was obtained and plotted on Fig. 5. That is, each long recording period was broken up into several shorter periods of various lengths, and the variance among medians of groups of hourly medians was determined for each of several sample sizes. As an example, for n = 36 days, Fig. 5 reads $\sigma_{oo}^2(50) = 19.6\ db^2$; this is the variance of the medians of five groups of 180 hourly medians each, representing five 36-day recording

periods. Actually, the figure shows averages of values obtained for a number of paths in Time Block 2, winter afternoons. The shape of the variance curve for other time blocks was not found to be significantly different. The level of $\sigma_{oo}^2(50)$ for n = 0.2 was determined from the estimates of long-term variability for all hours as given in Fig. 4, assuming that n = 0.2 corresponds to one hour, as it does for Time Block 2. Fig. 5 also contains a curve for the weight $w_{oo}(50)$, the reciprocal of $\sigma_{oo}^2(50)$, as a function of n. This weight curve is added for convenience, if needed directly in calculations.

Available data indicate that the variances $\sigma_o^2(50)$ are much more a function of angular distance than the prediction uncertainty σ_c^2 discussed in Sec. 6 of Ref. 1, and shown here on Fig. 1. Curves of $\sigma_o^2(50)$ versus n for various angular distances are roughly parallel, and their mutual relation corresponds approximately to the $V(p, \theta)$ curves shown on Figs. 2, 3 and 4. A factor $f(\theta)$ has been determined on the basis of the all day-all year $V(p, \theta)$ curves, by which the variance $\sigma_{oo}(50)$ shown on Fig. 5 corresponding to an angular distance of 18.2 milliradians has to be multiplied to obtain the variance $\sigma_o^2(50)$ for a given angular distance θ. The factor $f(\theta)$ as a function of θ is shown on Fig. 6, and the relation may be expressed by the equation

$$\sigma_o^2(50) = \sigma_{oo}^2(50)f(\theta) \qquad (8)$$

The following paragraphs explain how the variance $\sigma_o^2(p)$ is obtained for values of p other than 50%. Here, $\sigma_o^2(p)$ is the variance of observed hourly median field strength values $E_o(p)$ exceeded for p% of all hours.* On the average, $E_o(p)$ and $L_{bo}(p)$ are related to $E_o(50)$ and $L_{bo}(50)$ as shown in (7) above:

$$E_o(p) = E_o(50) + \Delta V(p, \theta), \qquad (9)$$

or

$$L_{bo}(p) = L_{bo}(50) - \Delta V(p, \theta) \qquad (9a)$$

where

$$\Delta V(p, \theta) = V(p, \theta) - V(50, \theta) \qquad (10)$$

It should be noted that here $E_o(50)$ or $L_{bo}(50)$ refers to the median of the time block or time block group considered. It is also assumed that errors in $E_o(50)$ and $\Delta V(p, \theta)$ are uncorrelated, and that the variance $\sigma_{\Delta V}^2(p)$ is proportional to $(\Delta V)^2$:

$$\sigma_{\Delta V}^2(p) = k^2(\Delta V)^2 \qquad (11)$$

It follows that $\sigma_o^2(p)$ may be written

*Again, a field strength value E(p) exceeded during p% of all hours is equivalent to a transmission loss value L(p) not exceeded during the same p% of all hours.

$$\sigma_o^2(p) = \sigma_o^2(50) + k^2(\Delta V)^2 \qquad (12)$$

where $\sigma_o^2(50)$ is obtained from (8), using Figs. 5 and 6, while ΔV is obtained from Fig. 2, 3 or 4, whichever is applicable to the measurement period considered.

The reasonableness of the above assumptions was verified and a value of 0.09 for k^2 was determined using the same Ohio data discussed in the appendix to Ref. 1. Certain parameters for these data are listed in Table II, which gives values of $\sigma_o^2(50)$ determined from (8) for each of two frequencies and two distance ranges.

The number of days of measurement shown in Col. 6 of Table II represents a full year of random sampling at 125 miles and seven months of random sampling at 85 miles.

Observed values of $\sigma_o^2(p)$ for each set of data were normalized to agree at p = 50% with the theoretical value listed in Table II by adding or subtracting an appropriate variance. These normalized variances $\sigma_o^2(p)$ for the four sets of data were then averaged; these averages are listed in Table III. The $V(p, \theta)$ values in Table III are based on the average θ = 25.7 milliradians for all paths.

Table II

Data for Determination of $\sigma_o^2(50)$

Station Call Letters	Freq. in Mc	Nominal Distance in mi.	Average Angular Distance θ in Milliradians	$f(\theta)$ from Fig. 6	No. of Days (Approx.)	$\sigma_{oo}^2(50)$ from Fig. 5	$\sigma_o^2(50)$ from (8)	Observed values of $\sigma_o^2(50)$
WCOL	92.3	125	27.8	0.59	52	16.8	9.91	8.48
WCOL	92.3	85	24.4	0.69	24	23.7	16.35	20.50
WHKC	98.7	125	26.5	0.625	54	16.3	10.18	6.57
WHKC	98.7	85	24.1	0.70	31	21.0	14.70	19.88

Table III

	p				
	1%	10%	50%	90%	99%
$\sigma_o^2(p)$	37.59	19.61	12.74	21.22	29.54
$V(p, \theta)$ (from Fig. 4)	22.2	13.0	3.8	- 4.0	-10.2
ΔV (from (10))	18.4	9.2	0	- 7.8	-14.0
k^2 (from (12))	0.0734	0.0812	-	0.1394	0.0856
k	0.271	0.285	-	0.373	0.293
$\rho(p)$ (from (13) below)	- 0.18	- 0.06	-	+ 0.16	- 0.06

The average value of k^2 in Table III is approximately 0.09, as determined by assuming no correlation between errors in $E_o(50)$ and ΔV. If the value of k is fixed at 0.3 and it is assumed that $\sigma_{\Delta V} = k|\Delta V|$, then the calculated correlation coefficient $\rho(p)$, using the data of Table III, is seen to be essentially zero at each percentage level. For this calculation, the relation

$$\sigma_o^2(p) = \sigma_o^2(50) + \sigma_{\Delta V}^2(p) + 2\rho(p)\sigma_o(50)\sigma_{\Delta V}(p) \qquad (13)$$

was used.

Thus (12) is justified, with 0.09 as the value for k^2.

Recapitulating, we now have an estimate of the variance $\sigma_o^2(p)$ to

be assigned to a measured field strength value $E_o(p)$ exceeded by p% of all hourly medians. Combining (9), (10) and (12):

$$\sigma_o^2(p) = \sigma_{oo}^2(50)f(\theta) + 0.09[V(p, \theta) - V(50, \theta)] \qquad (14)$$

where Figs. 5 and 6 and one of the appropriate curves of Figs. 2, 3 or 4 are used to evaluate $\sigma_o^2(p)$ from (14).

The preceding paragraphs in this section assume that measurements are made in the same time block for which estimates are desired. It will usually be the case that measurements will be made for a period of weeks or months either in summer or winter, and that estimates will be desired for all year. A generalization of (12) is here made which depends upon a generalization of (9) or (9a) inherent in prediction methods described in Ref. 5. Suppose we have available a measured cumulative distribution for the summertime and desire estimates of L(p) for all year. Denote by $V_S(p, \theta)$ the function $V(p, \theta)$ plotted in Fig. 3 for the summer months May through October, and denote by $V_A(p, \theta)$ the function $V(p, \theta)$ plotted for all hours in Fig. 4. Then re-define ΔV as follows; with the double subscript denoting that it is the difference between a $V(p, \theta)$ value, $V_A(p, \theta)$ in time block group A (all year), and a $V(p, \theta)$ value, $V_S(p, \theta)$ in time block group S (summer):

$$\Delta V_{AS} \equiv \Delta V_{AS}(p, \theta) = V_A(p, \theta) - V_S(p, \theta) \qquad (15)$$

An estimate of $L_{bA}(p)$ for all hours is obtained from the measured value of $L_{bS}(p)$ using the following relation:

$$L_{bA}(p) = L_{bS}(p) - \Delta V_{AS}(p, \theta) \tag{16}$$

This is the analog to (8b), and (10) may be rewritten for the summer period:

$$\Delta V_S \equiv \Delta V_S(p, \theta) = V_S(p, \theta) - V_S(50, \theta) \tag{10a}$$

Our extension of (12) is then

$$\begin{aligned} \sigma_o^2(p) \equiv \sigma_{AS}^2(p) &= \sigma_o^2(50) + k^2 [(\Delta V_S)^2 + (\Delta V_{AS})^2] \\ &= \sigma_{oo}^2(50) f(\theta) + 0.09\{[V_S(p, \theta) - V_S(50, \theta)]^2 \\ &+ [V_A(p, \theta) - V_S(p, \theta)]^2\} \end{aligned} \tag{17}$$

Equation (17) now replaces (14), which it generalizes, so that a weight $w_o(p)$ may be assigned to an $L_{bA}(p)$ obtained by correcting a measurement $L_{bS}(p)$ made in the summertime. Equation (16) is used to estimate a value for all year from measurements made during part of the year. If measurements are made in the winter, change the subscript S to F in the preceding equations and use Fig. 2 instead of 3. In cases where measurements are made during individual time blocks only, the appropriate $V(p, \theta)$ curves from Ref. 5 have to be used instead of Figs. 2, 3 or 4.

4. Application of the Standard Deviation $\sigma_{oe}(p)$ to Predictions, and Prediction Improvement

The standard deviations $\sigma_o(p)$ calculated in accordance with the methods given in the preceding section characterize the prediction uncertainty associated with any observed field strength or transmission loss value if the observed value is not subject to equipment or reading errors. Section 3 introduced the symbol σ_e to characterize such errors, considered to be independent of the measured field strength or transmission loss value. Under the reasonable assumption that the prediction uncertainty and the equipment errors are uncorrelated, the weight $w_o(p)$ assigned to an observed value $L_{bo}(p)$ is is given by

$$\frac{1}{w_o(p)} = \sigma_{oe}^2(p) = \sigma_o^2(p) + \sigma_e^2 \qquad (6a)$$

For the usual transmission loss measurement and analysis procedures, a value of 2 decibels constitutes a good estimate of σ_e.

As the standard deviation $\sigma_{oe}(p)$ now characterizes the uncertainty associated with the observed value $L_{bo}(p)$ for each percentage point p, it may be used directly to draw a service probability graph in accordance with the method described in Ref. 1. This means that the performance of a system may be estimated on the basis of measurements alone without any calculation of basic transmission loss at all. For this procedure it is only necessary to modify $\sigma_{oe}(p)$ by

taking into account the uncertainty in estimating system equipment parameters just as was done in the theoretical prediction case (see p. 10 of Ref. 1). The total uncertainty $\sigma_{or}(p)$ in this case is given by an equation analogous to (4) of Ref. 1:

$$\sigma_{or}^2(p) = \sigma_{oe}^2(p) + \sigma_r^2, \qquad (18)$$

where σ_r, usually taken as 2 decibels, characterizes the uncertainty in estimating system equipment parameters. Service probabilities may now be calculated in accordance with (5) and (6) of Ref. 1. Observed transmission loss values $L_{bo}(p)$ are related to system power requirements by appropriate constants depending on the grade of service required if all quantities are expressed in decibels. A convenient expression for this is given by Norton[7],

$$P_{to} = L_{bo} - G_p + F + L_t + R + B - 204 \qquad (19)$$

where

P_{to} = transmitter power in decibels relative to one watt

L_{bo} = basic transmission loss over the path in decibels

G_p = path antenna gain in decibels

F = effective receiver noise figure in decibels

7/ K. A. Norton, "Point-to-point radio relaying via the scatter mode of tropospheric propagation," Trans. IRE on Comm. Systems, Vol. CS-4, No. 1, pp. 39-49, March 1956

L_t = transmission line and associated losses, in decibels

R = pre-detection r.m.s. carrier to r.m.s. noise ratio in decibels, for the bandwidth, type of modulation, and order of diversity used

B = $10 \log_{10} b$, where b is the total bandwidth in cycles per second (including the effect of drift between transmitter and receiver oscillators)

204 = a constant equal to $-10 \log_{10} kT$, where k is Boltzmann's constant, and the reference temperature T is taken to be 288.44^{o} Kelvin

The usual procedure is to utilize measurements in conjunction with predictions, in order to reduce the prediction uncertainty. Recapitulating the results obtained in Section 2 above, it is necessary to distinguish cases where measurements are available for exactly the same path for which the prediction is desired from the ones where the paths are similar, or in the same general area.

In the first case, the improved prediction is given by (1). It may be re-written in terms of basic transmission loss values:

$$L_{bt}(p) = \frac{w_o(p)L_{bo} + w_c(p)L_{bc}}{w_o(p) + w_c(p)} \qquad (1a)$$

The weight and the variance assigned to the improved prediction $L_{bt}(p)$ is given by

$$w_t(p) = \frac{1}{\sigma_t^2(p)} = w_o(p) + w_c(p) \qquad (20)$$

with $w_c(p)$ shown on Fig. 1 as a function of p.

$\sigma_t(p)$ is a measure of the remaining prediction uncertainty characteristic of the improved basic transmission loss values $L_{bt}(p)$ just as $\sigma_c(p)$ was a measure of the original prediction uncertainty pertaining to the theoretical values $L_{bc}(p)$. If system power requirements are considered, the term σ_r^2 has to be added to $\sigma_t^2(p)$ in order to obtain a measure of the remaining total prediction uncertainty taking into account the uncertainty in estimating the system parameters F and R as discussed on p. 10 of Ref. 1. Thus, the remaining prediction uncertainty is characterized by a standard deviation $\sigma_t(p)$ as a function of p, if hourly medians of transmission loss or field strength values are considered, or by a standard deviation $\sigma_{tr}(p)$, if predictions are to be made for the performance of a complete system. $\sigma_{tr}(p)$ is given by

$$\sigma_{tr}^2(p) = \sigma_t^2(p) + \sigma_r^2 \qquad (21)$$

For the second case, where measurements are available for one path (Path a), whereas a prediction is desired for another path (Path b), the improved prediction on the basis of measurement for Path a and its variance is first determined in accordance with (1a) and (20) above. To this improved prediction L_{bta}, the difference of the calculated values L_{bca} and L_{bcb} for the two paths is added as in (2) in Sec. 2 above:

$$L_{btb} = L_{bta} + (L_{bca} - L_{bcb}) \qquad (2a)$$

The variance σ_{tb}^2 characterizing L_{btb} is now obtained in accordance with (5) using an appropriate assumption for the correlation coefficient ρ_{ab}. For the design of a system, the variance σ_r^2 has to be added to σ_{tb}^2, as in (21).

$$\sigma_{trb}^2(p) = \sigma_{tb}^2(p) + \sigma_r^2 \qquad (21a)$$

Having obtained $L_{bt}(p)$ or $L_{btb}(p)$ and $\sigma_{tr}(p)$ or $\sigma_{trb}(p)$ as functions of p, service probability values may be calculated in the same way as was done for the theoretical prediction described in Ref. 1.

The procedure will be demonstrated by examples in the next section.

5. Examples

In this section the prediction improvement method is illustrated by the use of two examples. In the first example, measurements made over a 200-mile path between North Africa and Spain are used to demonstrate prediction improvement. This is the sample path discussed in Ref. 1. The second example illustrates the effect of increasing the length of the measurement period, and a portion of long-term measurement results (data obtained from an FM broadcasting

station in the U. S.) is used.

(a) Prediction Improvement for the Sidi Slimane-Moron Path

The results of transmission loss measurements over this path have been described previously[8,9]. In order to improve the prediction for the operation in the 700-900 Mc range used as examples in Ref. 1, the 17 days of measurements over exactly the same path (Sidi Slimane Relay Center to Moron Site A) on 1046 Mc were utilized. For the purpose of this example it is assumed that the difference in frequency is not great enough to make the paths significantly different, i.e., ρ_{ab} is assumed to be equal to 1. The measured distribution of hourly median values of basic transmission loss is shown by the dotted line on Fig. 7, designated as $L_{bo}'(p)$. The measurements were made in February of 1957 during all hours and thus represent time block group F (Time Blocks 1, 2, 3 and 8).

In accordance with (16) of Sec. 3, above, the measured values are adjusted to all day-all year values by subtracting the term $\Delta V_{AF}(p, \theta)$. This term, given by (15), is the difference between the $V(p, \theta)$ values for all day-all year (read from Fig. 4 at the path angular distance value θ = 40.3 milliradians), and the $V(p, \theta)$ values

---

8,9/ A. P. Barsis and R. S. Kirby, "Long distance tropospheric propagation measurements between North Africa and Spain," NBS Reports 5067 and 5524, May 15 and October 15, 1957

for all hours-winter (read from Fig. 2 at the same θ = 40.3 milliradians). The adjusted values, $L_{bo}(p)$, are shown by the broken line on Fig. 7. This curve represents the observed values. The weight assigned to the median $L_{bo}(50)$ is obtained from (9), using Figs. 5 and 6. For n = 17 days, $\sigma_{oo}^2(50) = 27.1\ (db)^2$, and for θ = 40.3 milliradians, $f(\theta) = 0.398$. Thus $\sigma_o^2(50)$ is determined to be $10.79\ (db)^2$. Values of $\sigma_o^2(p)$ are now determined for other percentage values in accordance with (17) using the differences of the appropriate $V(p, \theta)$ values from Figs. 2 and 4, as before. To each $\sigma_o^2(p)$ a term $\sigma_e^2 = 4.0\ (db)^2$ is added in order to allow for equipment (reading and calibration) errors. The resultant values $\sigma_{oe}(p)$ represent the uncertainty assigned to each observed value $L_{bo}(p)$, as adjusted to all day-all year values. The weight $w_o(p)$ assigned to each value $L_{bo}(p)$ is the reciprocal of $\sigma_{oe}^2(p)$.

For the same 1046 Mc frequency, the Time Block 2 median (of hourly medians) basic transmission loss value is read from Fig. 2 of Ref. 1, as the sample calculations of Ref. 1 refer to the same path. This value, L_{bm} = 214.7 db, together with the $V(p, \theta)$ values of Fig. 4, produces the calculated distribution of hourly medians for all day-all year:

$$L_{bc}(p, \theta) = L_{bm} - V(p, \theta) \qquad (22)$$

The calculated values $L_{bc}(p, \theta)$ are shown by the dash-dotted line on Fig. 7. They may be redesignated as $L_{bc}(p)$, as the angular

distance θ has now been fixed. The prediction uncertainty $\sigma_c(p)$ associated with each $L_{bc}(p)$ is given by curve (a) of Fig. 1, as there is no significant contribution of the diffracted field over this path, and, prior to combining predictions and measurements, the system error σ_r (representing principally the uncertainties in estimating the system parameters F and R) does not enter. The weights $w_c(p) = 1/\sigma_c^2(p)$ are shown on Fig. 1.

Now the weighted average of $L_{bc}(p)$ and $L_{bo}(p)$ may be obtained in accordance with (1a), resulting in the distribution of hourly medians $L_{bt}(p)$, the improved prediction. This is the solid curve on Fig. 7, and the corresponding weights $w_t(p)$ are obtained by adding $w_c(p)$ and $w_o(p)$.

The performance of a communication system utilizing this path may now be predicted on the basis of three methods: first, using the calculated values alone; second, using only observed values; and third, using the weighted average of the two, which constitutes the improved prediction.

The first case has already been discussed in Ref. 1. For this case the distribution $L_{bc}(p)$ of Fig. 7 is used with the prediction uncertainty given by the dash-dotted $\sigma_{rc}(p)$ curve of Fig. 8, which is the same curve as the (b) curve of Fig. 1. The system error σ_r is included in $\sigma_{rc}(p)$.

$$\sigma_{rc}^2(p) = \sigma_c^2(p) + \sigma_r^2 \qquad (23)$$

For the second case the observed distribution (adjusted to all day-all year) $L_{bo}(p)$ of Fig. 7 is used, together with the prediction uncertainty $\sigma_{or}(p)$ shown by the dashed curve on Fig. 8. As the prediction applies to a complete system, $\sigma_{or}(p)$ also contains the system error σ_r:

$$\sigma_{or}^2(p) = \sigma_{oe}^2(p) + \sigma_r^2 \qquad (23a)$$

Finally, the improved prediction curve $L_{bt}(p)$ of Fig. 7 is used together with the prediction uncertainty $\sigma_{tr}(p)$ shown by the solid curve on Fig. 8. Again, $\sigma_{tr}(p)$ contains the system error σ_r, and is given by

$$\sigma_{tr}^2(p) = \sigma_t^2(p) + \sigma_r^2 \qquad (23b)$$

where $\sigma_t^2(p)$ is the reciprocal of the sum of the weights $w_o(p)$ and $w_e(p)$ in accordance with (20).

Fig. 8 shows that the prediction uncertainty is appreciably reduced by the use of these measurements. Note that the distribution of the observed hourly median values shown on Fig. 7 indicates substantially lower fields at the high percentage values than would be

expected from the values calculated on the basis of the $V(p, \theta)$ curves of Fig. 4.*

As the last step, service probability curves will be calculated in accordance with the methods of Ref. 1. In this particular case, the effects of higher transmission loss and lower prediction uncertainty values tend to balance each other, as seen by the final comparison of service probabilities for 99 or 99.9% of all hours for the three cases.

It was explained in Ref. 1 that the system power $P[F(t), p]$ required to provide the specified grade of service or better during p% of all hours with the probability $F(t)$ is related to the expected value of system power $P(0.5, p)$ by

$$P[F(t), p] = P(0.5, p) + t \cdot \sigma(p) \qquad (24)$$

where $P(0.5, p)$ here relates to the three curves of basic transmission loss values $L_{bc}(p)$, $L_{bo}(p)$, and $L_{bt}(p)$, and $\sigma(p)$ is identical to either $\sigma_{rc}(p)$, $\sigma_{or}(p)$, or $\sigma_{tr}(p)$ depending on the three cases considered. For the same system as used in Ref. 1 (60 ft. parabolic reflectors, quadruple diversity FM, 850 Mc carrier frequency), and the same specified grade of service (24 voice channels, several of which are

* It should be noted that the original measured distribution (Fig. 3 of Ref. 7) has been smoothed and extrapolated in order to facilitate the calculations.

loaded with standard frequency-shift teletype signals with less than 1 in 10,000 character errors) it can be shown by substitution into (19) that the required transmitter power P_t in decibels above one watt is given by the hourly median basic transmission loss L_b minus 197 db. Thus a fixed transmitter power P_o = 1 kw (30 dbw) corresponds to 227 db basic transmission loss on the curves of Fig. 7, and P_o = 10 kw (40 dbw) corresponds to L_b = 237 db. Substituting P_o for $P[F(t), p]$ in (23) and solving for t,

$$t = \frac{P_o - P(0.5, p)}{\sigma(p)} \qquad (25)$$

and from t, the service probability F(t) may be found from appropriate probability tables[10].

For each of the three cases, F(t) may be now determined as a function of p, with $P(0.5, p)$ and $\sigma(p)$ read from the appropriate curve of Figs. 7 and 8, and for P_o fixed at 1 or 10 kw. The resultant curves of service probability are shown on Fig. 9.

The curves on Fig. 9 show the anticipated results, namely that the decrease in the prediction uncertainty is not sufficient to compensate for the effect of the low values of field measured during an appreciable percentage of the time. Only on the basis of a 0.99

10/ C. A. Bennett and N. L. Franklin, "Statistical analysis in chemistry and the chemical industry," John Wiley and Sons, Inc., New York, 1954. See p. 86 and Table I of the Appendix (pp. 689-693)

service probability (only 1 out of 100 chances of failure) do the measurements indicate a greater time availability of service than is indicated by the prediction alone. This applies to the use of 1 kw transmitter power. The analysis suggests that for this particular example the use of the calculated values alone would probably lead to results that were too optimistic, especially if lower values of service probability (0.5 to 0.8) had been the basis for the estimates.

A more direct comparison may be made by fixing F(t) and p, and solving for P_o in (25); this shows the transmitter power necessary to provide the specified grade of service, or better, during p% of all hours with a given probability of success F(t). If this is done for the sample path and the system considered, the following results are obtained:

Table IV

	Transmitter Power in Decibels Relative to 1 Watt
(a) F(t) = 0.95, p = 99%	
Calculated only	38.5
Observed only	45.1
Improved prediction	39.7
(b) F(t) = 0.99, p = 99%	
Calculated only	40.3
Observed only	48.9
Improved prediction	42.9
(c) F(t) = 0.99, p = 99.9%	
Calculated only	48.1
Observed only	55.1
Improved prediction	48.2

In Table IV, (a) corresponds to a 0.95 probability (1 out of 20 chances of failure) to obtain the specified grade of service or better during 99% of all hours. For (b) the probability is increased to 0.99 (only 1 out of 100 chances of failure), and for (c) the percentage of hours is increased to 99.9%, representing together with the 0.99 service probability a virtually perfect circuit. In each case the required transmitter power would be substantially higher if based on the analysis of the limited observations only. The results, based on the predicted values improved by the measurement, are not very different from the results based on the use of the calculated predicted values alone.

For the path and the system under discussion, therefore, the measurements did not add significantly to the information gained from theoretical considerations alone, and estimates based on the use of the measurement alone would have been entirely too pessimistic. These conclusions, of course, apply to service fields, where a high degree of reliability during the greatest percentage of hours of the year is desired. The findings would have been quite different in the consideration of nuisance or interference fields for this path.

(b) Prediction Improvement for the St. Louis-Urbana Path

Field strength measurements on broadcasting station KXOK-FM were made over the period July 1950 to June 1952 at Urbana, Illinois. This is one of the paths listed in Appendix IV of a

previous comprehensive paper on the use of angular distance in transmission loss calculations[6]; the path distance is 146.5 miles, the angular distance 19.3 milliradians, and the operating frequency 93.7 Mc.

In order to investigate prediction improvement as a function of the length of the measurement period, the following nominal time periods were selected from the KXOK data:

Nov. 1 - 7, 1950	7 days
Nov. 1 - 15, 1950	15 days
Nov. 1 - 30, 1950	30 days
Nov. 1 - Dec. 31, 1950	60 days
Nov. 1, 1950 - Apr. 30, 1951	180 days
Nov. 1, 1950 - Oct. 31, 1951.....	365 days

For each period all available hourly medians were used, thus all but the 365-day period represent the winter time block group F, and the 365-day period represents all hours of the year. It may be assumed that a measurement program was started on Nov. 1, 1950, and successively longer periods of measurement were used for the purpose of prediction improvement. Fig. 10 shows the measured distributions of hourly medians of basic transmission loss for the first four periods tabulated above, and Fig. 11 the measured and theoretical distributions for the full time block group F (all hours, winter), and for all

hours of the year. The theoretical distributions were obtained from Figs. 2 and 4 using the calculated Time Block 2 median basic transmission loss value of 179.2 db as the reference value, L_{bm}. This, in turn, was calculated in accordance with the method given in Ref. 5.

Using the same procedure as in the previous example, measured distributions were adjusted to all day-all year values, and combined with the calculated all day-all year distribution.

The following table lists $\sigma_o^2(50)$ versus n derived from Figs. 5 and 6 for this path, with $f(\theta) = 0.93$:

Table V

Number of days n	$\sigma_{oo}^2(50)$ db	$\sigma_o^2(50)$ db
7	38.85	36.1
15	28.7	26.7
30	21.2	19.7
60	15.7	14.6
180	9.4	8.75
365	6.7	6.25

The resultant improved prediction curves of the expected distributions of hourly medians are shown on Fig. 12 taking into account all six measurement periods. The appropriate standard deviations σ_{tr} characterizing the remaining prediction uncertainties are shown on Fig. 13. Each of the curves is labeled with the number of

days contained in the measurement period utilized. The standard deviation σ_{tr} in each case contains the component σ_r, as in the previous example, in order to take system performance uncertainties into account. It is to be kept in mind that the measurements would ultimately be used to estimate the performance of a communication system.

For the purpose of illustrating the problem it is sufficient to assume that one single value of hourly median basic transmission loss on the curves of Figs. 11 or 12 characterizes a system with a fixed transmitter power value P_t. The value chosen for the example is 190 db, and it is taken as the basis for service probability calculations. For each of the $L_{bt}(p)$ curves of Fig. 12, the appropriate $\sigma_{tr}(p)$ curve (for the same number of days) of Fig. 13 is used. The resulting service probability curves are shown on Fig. 14; they are again labelled with the number of days to which they apply. Fig. 14 also includes the service probability curve for calculated values alone (without taking into account the measurements). These are based on the same 190 db value of basic transmission loss characterizing the assumed system, and were developed using the calculated all day-all year distributions of Fig. 11 with the $\sigma_{rc}(p)$ standard deviation curve of Fig. 8.

As in the previous example, any of the service probability curves in Fig. 14 is affected not only by the remaining prediction uncertainty expressed by the standard deviation $\sigma_{tr}(p)$, but also by the shape of the appropriate $L_{bt}(p)$ curve, and thus by the measured distribution of hourly medians. Figs. 10, 11 and 12 show that the first 60 days of measurement did not produce enough high transmission loss (low field strength) values to pull the curves down sufficiently in the high percentage range. Only for the longer measurement periods the improved prediction takes into account those low field strength values. The standard deviation $\sigma_{tr}(p)$, of course, decreases systematically inversely to the length of the measurement period, but does not always compensate for the low field strength values observed during the extended measurement period.

Summarizing some of these observations, two things happen to a service probability curve when additional measurements are taken into account. The slope of the curve decreases with the variance $\sigma_t^2(p)$, as more and more observations are taken into account. There is also a change in level of the service probability curves, depending on the behavior of the observed data. This change in level may be either up or down if additional data are added, as illustrated by the KXOK example. The combined effect of a change in slope and a change in level may be either an increase or a decrease in service probability

at a given value of time availability. The range of oscillation of these estimates of service probability will decrease as the number of measurements is increased. The Sidi Slimane-Moron example may very well represent an extreme departure from this expected trend. If, in that case, additional measurements had been performed comparable in extent to the KXOK example, a similar pattern for prediction improvement as a function of the length of the measurement period might have been recognized.

Returning to the KXOK example and Fig. 14, it is seen that for the service probability value of 0.95 any of the curves based on the improved prediction indicate a higher value of time availability than the curve based on calculated values alone.

As in the previous example, a comparison of basic transmission loss values (which directly correspond to system power) may be made for various lengths of the measurement period at fixed values of p and F(t). The results are outlined in the following table for F(t) = 0.95 and 0.99, and a time availability p of 99% and 99.9% of all hours.

Table VI

Equivalent Basic Transmission Loss in Decibels

		p = 99% F(t) = 0.95	p = 99% F(t) = 0.99	p = 99.9% F(t) = 0.99
Based on calculated values only		207.3	212.2	220.6
Based on improved prediction by measurement.....	7 days	201.3	205.4	211.7
	14 days	200.2	204.1	211.0
	1 month	200.5	204.3	211.5
	2 months	200.0	203.7	210.8
	6 months	200.7	204.4	211.8
	1 year	200.9	204.5	211.8

This particular example shows that the method of combining calculated and observed values may provide a substantial change in the prediction, with a 6 to 8 db reduction in transmitter power required to provide the specified grade of service during almost all hours of the year with a very high probability of success. In this case, it also appears that only 7 days of measurements are adequate to give this result, and the extension of measurement over the period of one full year does not provide much further change. On the other hand, some other seven-day period could have been selected with different results.

Of course, it must be remembered that all the measured field strength values for 90% of all hours or more were higher than the calculated ones. This is the opposite condition in comparison to

the other example. It may be concluded, generalizing from this example only, that a good indication of the prediction improvement may be obtained from only seven days of observation, while a larger measurement period serves only to confirm the result.

6. General Conclusions

As an extension of a method permitting evaluation of the probability of success of a tropospheric communication system on the basis of empirical parameters obtained from an extensive and very general measurement program, it has been shown how this prediction method may be modified to take into account transmission loss measurements over exactly the same path or a similar path for which the final system is intended. Of the two examples used to demonstrate the procedure, one indicates a substantial increase in time availability at a given level of prediction uncertainty as estimated using only a short period of measurements, while the other one does not indicate any significant change, taking account of measurements. In both examples it is shown that one has to be very careful in drawing conclusions from the results of measurement; the reduction in the prediction uncertainty does not always compensate for extreme departures of observations from the calculated values. The "improved prediction" obtained from forming a weighted average of calculated and observed values will always result in a reduction of the prediction uncertainty, because the resultant

weight is greater than each of the individual weights assigned to either the calculated or the observed values. However, the actual departure of calculated from observed field strength (or transmission loss values) plays an important part, as shown by the examples.

In some cases the designer or engineer wants to know whether to place reliance on an available set of measurements, or on a prediction formula. Thus it may be of interest to determine the expected number of days of measurement necessary to result in a prediction uncertainty equal to the prediction uncertainty associated with the calculated value. In terms of the preceding discussions, this means setting (17) equal to $\sigma_c^2(p)$ as given on Fig. 1 and solving for n, the number of days of measurements, as a function of the angular distance θ, and the time availability p in percent of all hours.

Several factors have to be recognized immediately:

1. A certain minimum number of hours (or days) is necessary to define a given percentage value for a distribution of hourly medians. As an example, it is necessary to have at least 50 hourly medians in order to define a 99% value.

2. If not more than 180 consecutive days of measurements are available, they may fall entirely within time block group F (winter) or S (summer). In this case, allowance has to be made in order to apply the results to all day-all year conditions.

3. The variance of the observed hourly medians is strongly dependent on the angular distance, θ, whereas the variance of the calculated hourly medians has so far been found to be practically independent of θ, at least for $\theta \geq 10$ milliradians, where the contribution of the diffracted field is negligible.

Thus we may write in accordance with (17), averaging the effect of the winter and the summer time block groups.

$$\sigma_{oe}^2(p) = \sigma_o^2(p) + \sigma_e^2 = \sigma_{oo}^2(50)\, f(\theta) + 0.09[(\Delta V_A)^2 + 1/2(\Delta V_{AF})^2 + 1/2(\Delta V_{AS})^2] \quad (26)$$

where:

$$\Delta V_A = V_A(p, \theta), - V_A(50, \theta) \quad (27)$$

$$\Delta V_{AF} = V_A(p, \theta) - V_F(p, \theta) \quad (27a)$$

$$\Delta V_{AS} = V_A(p, \theta) - V_S(p, \theta) \quad (27b)$$

The subscripts A, F, and S refer to all day-all year, the winter time block group and the summer time block group, respectively, with the $V(p, \theta)$ values read from Figs. 2, 3 or 4.

(26) is solved for $\sigma_{oo}^2(50)$ with p = 50, 90, 99 and 99.9% as a function of θ, and σ_e^2 assumed to be 4 db^2, by setting $\sigma_{oe}^2(p)$ equal to $\sigma_c^2(p)$; the latter being read from Fig. 1 for the various values of p used. The number of days, n, is then obtained from Fig. 5 as a

function of $\sigma_{oo}^2(50)$.

Results are plotted on Fig. 15, with the number of days, n, as ordinate versus the angular distance θ plotted as the abscissa. The curves shown are labelled with time availability in per cent of all hours. The results are interpreted in the following way; taking into account equipment (calibration and reading) errors, it takes, as an example, 10 days of continuous measurements to obtain a value of prediction uncertainty $\sigma_{oe}^2(99\%)$ at θ = 29 milliradians for 99% of all hours, which is equal to the prediction uncertainty $\sigma_c^2(99\%)$ assigned to the calculated value. In this particular example, the σ_c will be smaller than the $\sigma_{oe}^2(99\%)$ for any shorter measurement period; thus the calculated distribution of hourly medians would constitute a better estimate than a distribution obtained from observations over a shorter time period than 10 days. If the measurement period is longer than 10 days, the opposite is true, but in any event a still better estimate is provided by combining calculated and observed values in the manner described in this paper.

Fig. 15 should not be interpreted as indicating where and for how long measurements should be made. This question still depends on the relative cost of measurements versus, say, the cost of more transmitter power or larger antennas. If, for instance, the calculations for a particular path result in the requirement of 10 kw transmitters and

60 ft. parabolic reflectors, which would provide the specified grade of service or better with a probability of 0.95 during 99% of all hours, and if two weeks of measurements might be expected to show that 28 ft. antennas would provide a similar service probability, the designer will have to balance the cost of the measurements against the cost of installing and maintaining the larger antennas with due regard to the fact that the larger antennas would, in any case, provide a better service. Of course, there is always a possibility that measurements will show that more power, or larger antennas are required. In general, it is quite likely that measurements over a particular path will only serve to confirm the estimates made solely on the basis of calculations.

Although the basic concept of service probability and the methods for prediction and prediction improvement will always be valid, some changes in the detailed procedures are expected on the basis of additional data evaluation and interpretation. Work is in progress now to re-evaluate the long-term variability of hourly medians, and improve their reliability by allowing for the effect of frequency, especially at short distances. Also, it may turn out to be slightly better to replace the dependence on the angular distance θ by a dependence on antenna height and linear path distance. A better understanding of the factors underlying the long-term variability will ultimately result in a significant reduction of the prediction uncertainty.

7. Acknowledgements

The authors are indebted to Messrs. R. S. Kirby and J. W. Herbstreit for their careful review and their suggestions. Drafting work on the figures was done by Mr. J. C. Harman and his group. The manuscript was typed by Mrs. M. J. Benedict and Mrs. M. N. Olson.

ESTIMATED PREDICTION UNCERTAINTY FOR ALL HOURS
OF THE YEAR AS A FUNCTION OF THE PERCENTAGE OF HOURS

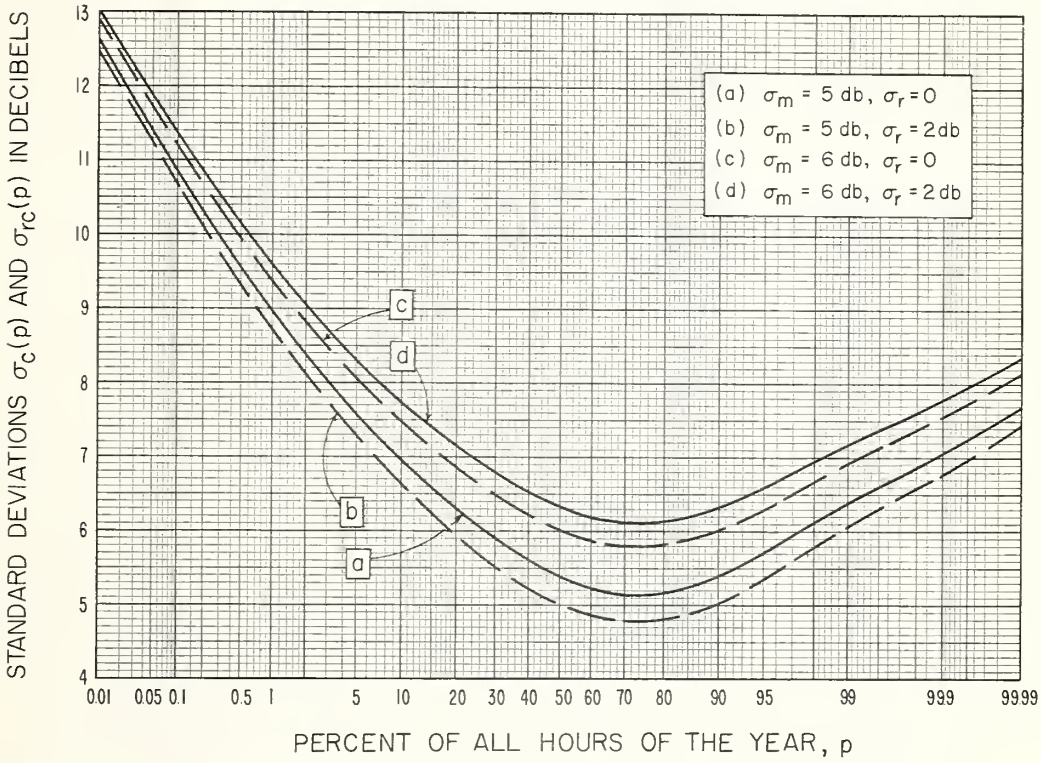

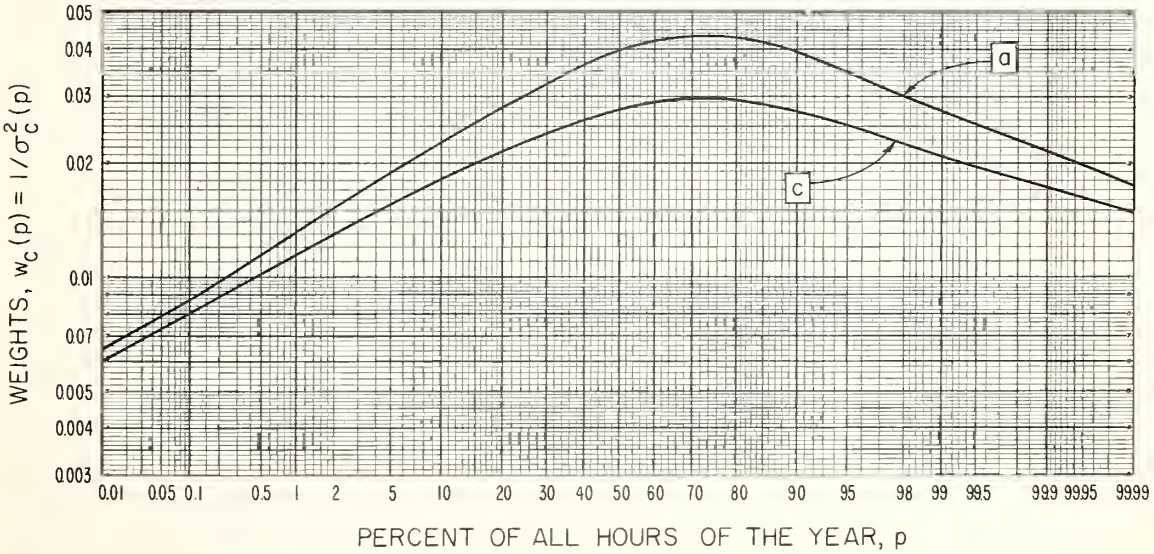

Figure 1

EXPECTED SIGNAL LEVEL, $V(p,\theta)$, EXCEEDED BY p PERCENT
OF ALL HOURS IN TIME BLOCK GROUP F
November — April, All Hours
$L_b(p,\theta) = L_{bm} - V(p,\theta)$ decibels

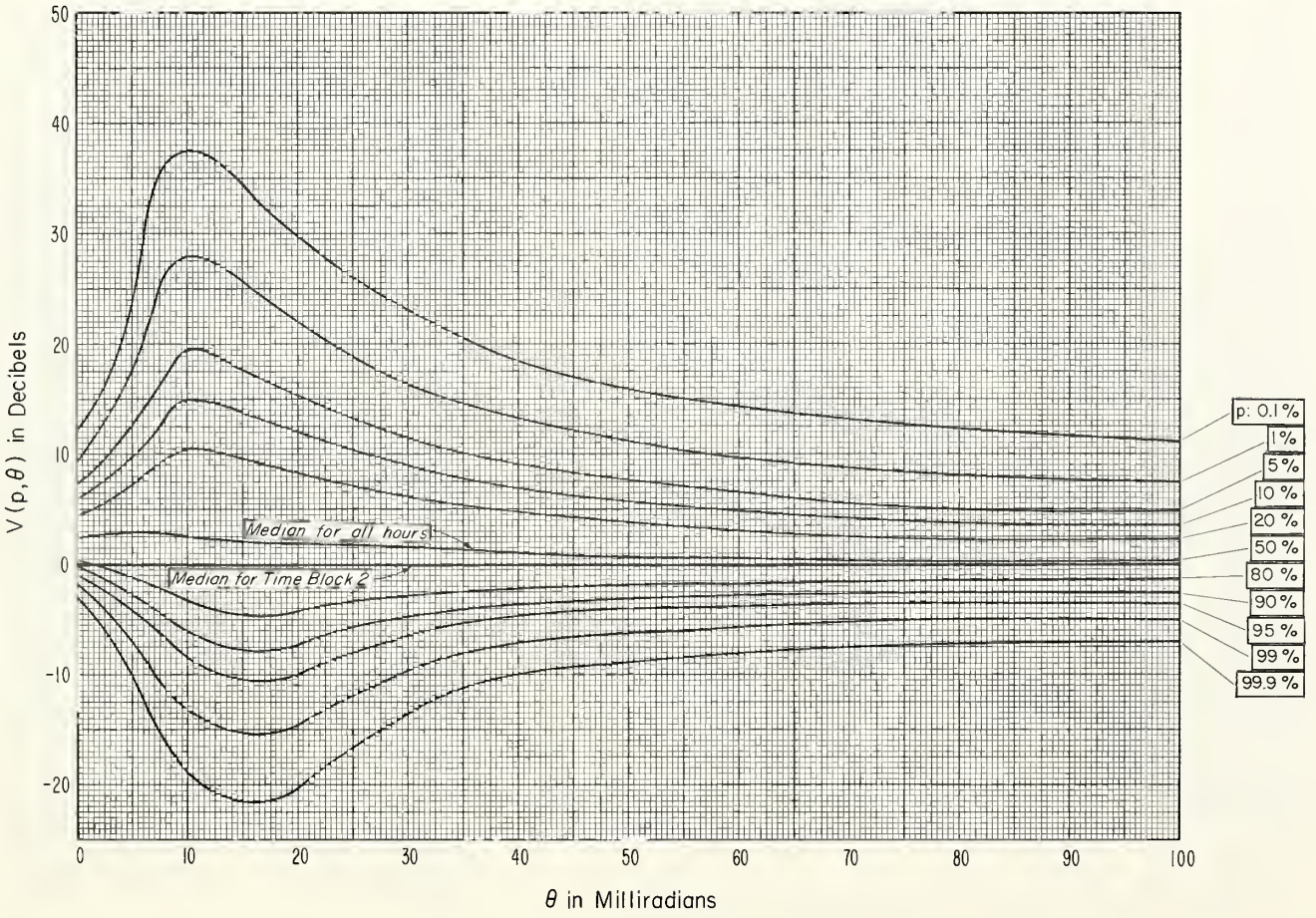

Figure 2

EXPECTED SIGNAL LEVEL, $V(p,\theta)$, EXCEEDED BY p PERCENT
OF ALL HOURS IN TIME BLOCK GROUP S
May - October, All Hours
$L_b(p,\theta) = L_{bm} - V(p,\theta)$ decibels

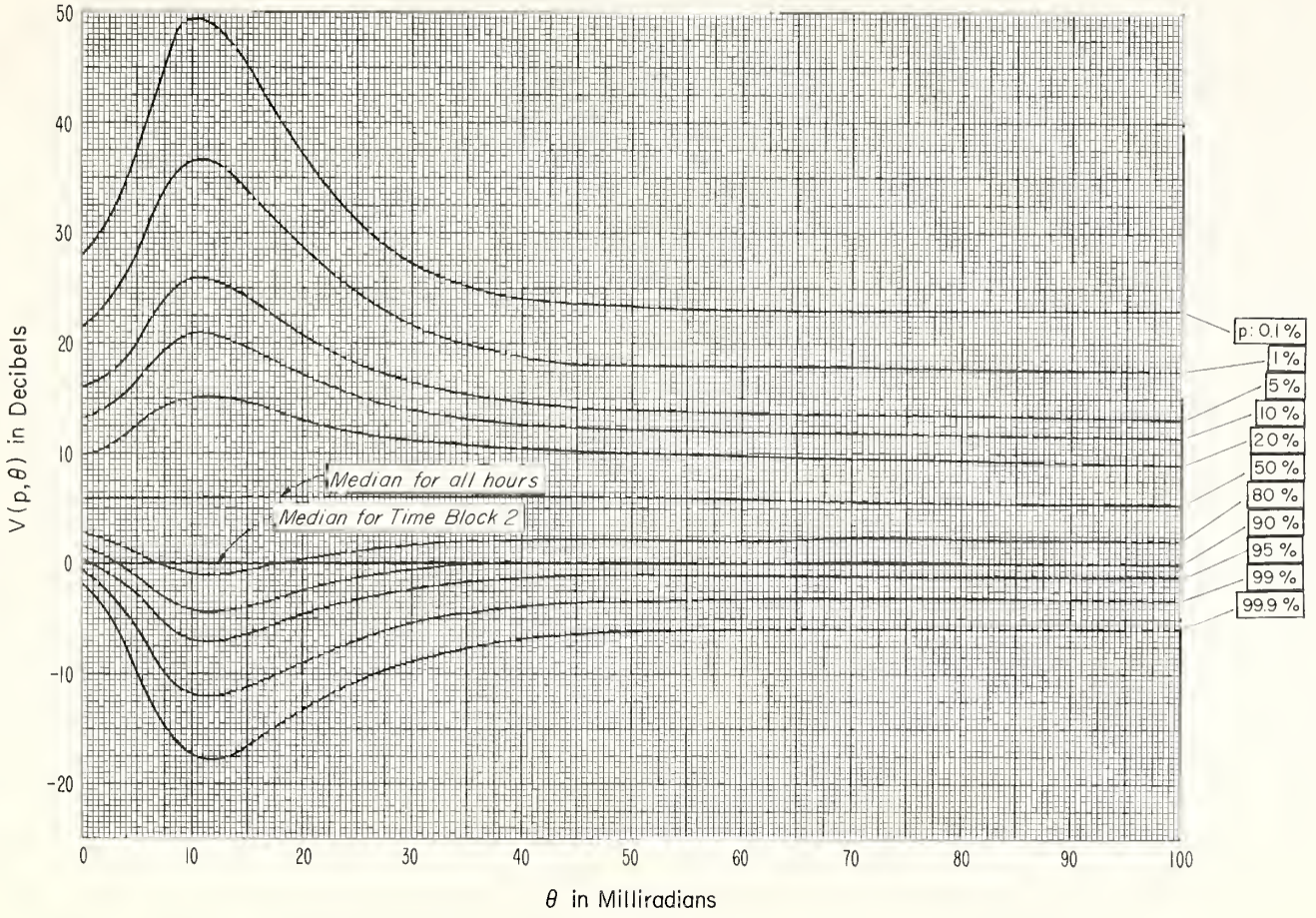

Figure 3

EXPECTED SIGNAL LEVEL, $V(p,\theta)$, EXCEEDED BY p PERCENT OF ALL HOURLY MEDIANS OBSERVED AT ANGULAR DISTANCE θ DURING ALL HOURS OF THE YEAR

$V(p,\theta)$ shows the deviation of all-day, all-year values, $L_b(p,\theta)$, relative to median basic transmission loss, L_{bm}, for the period November - April, 1 P.M. - 6 P.M. (Time Block No. 2)

$L_b(p,\theta) = L_{bm} - V(p,\theta)$ decibels

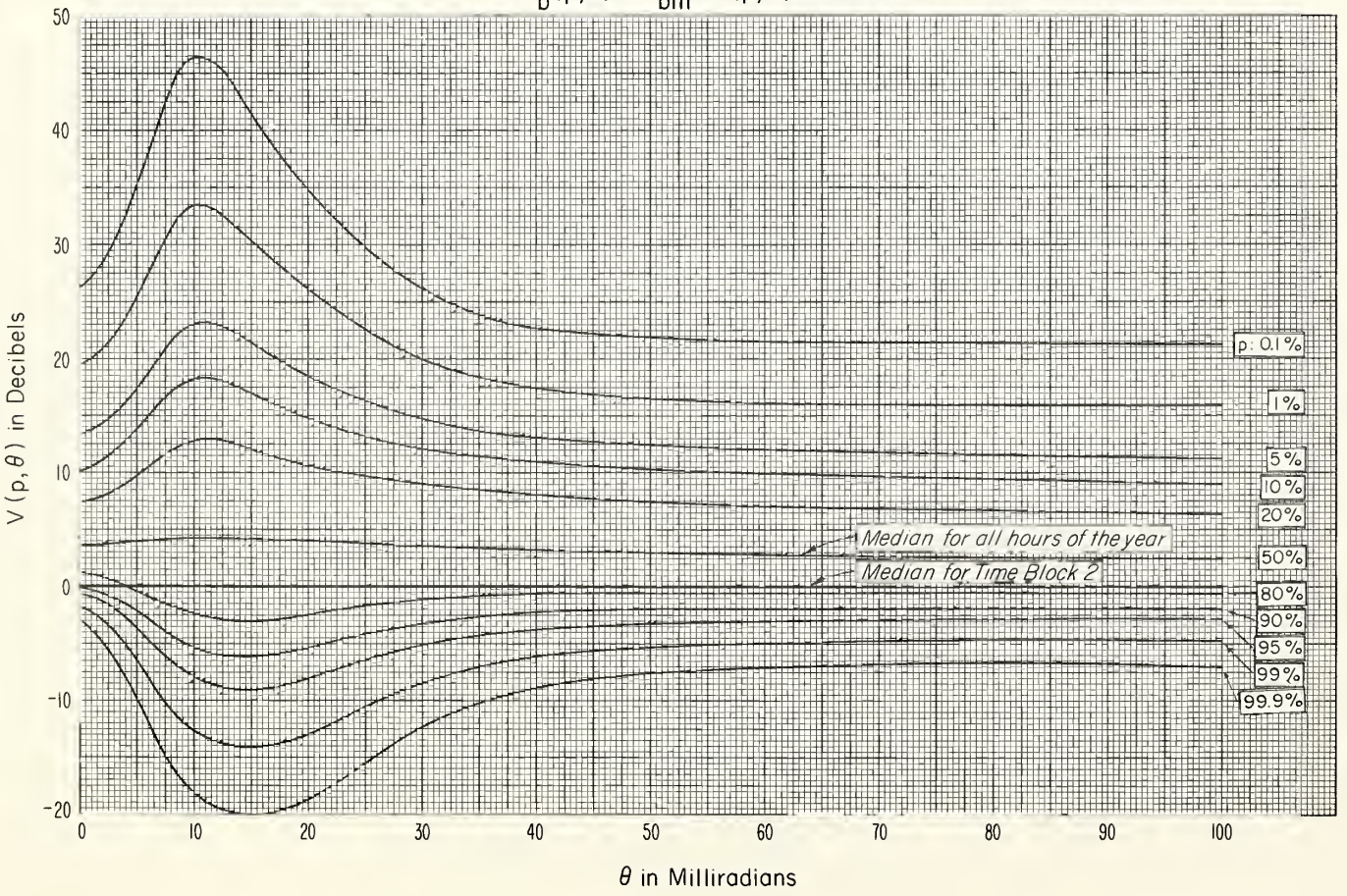

Figure 4

VARIANCES AND WEIGHTS FOR TIME BLOCK 2 MEDIANS
NORMALIZED TO θ = 18.2 mr

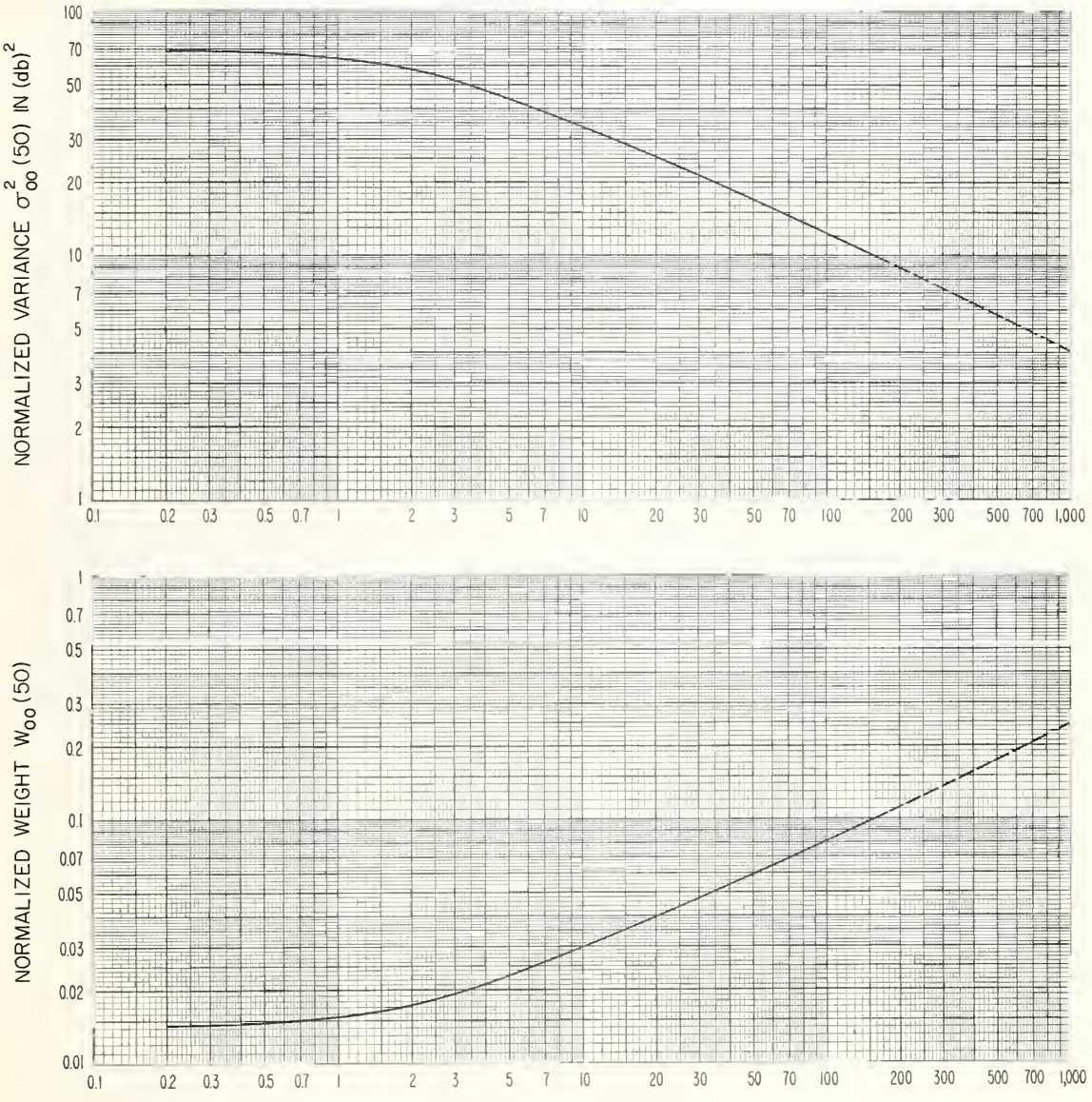

Figure 5

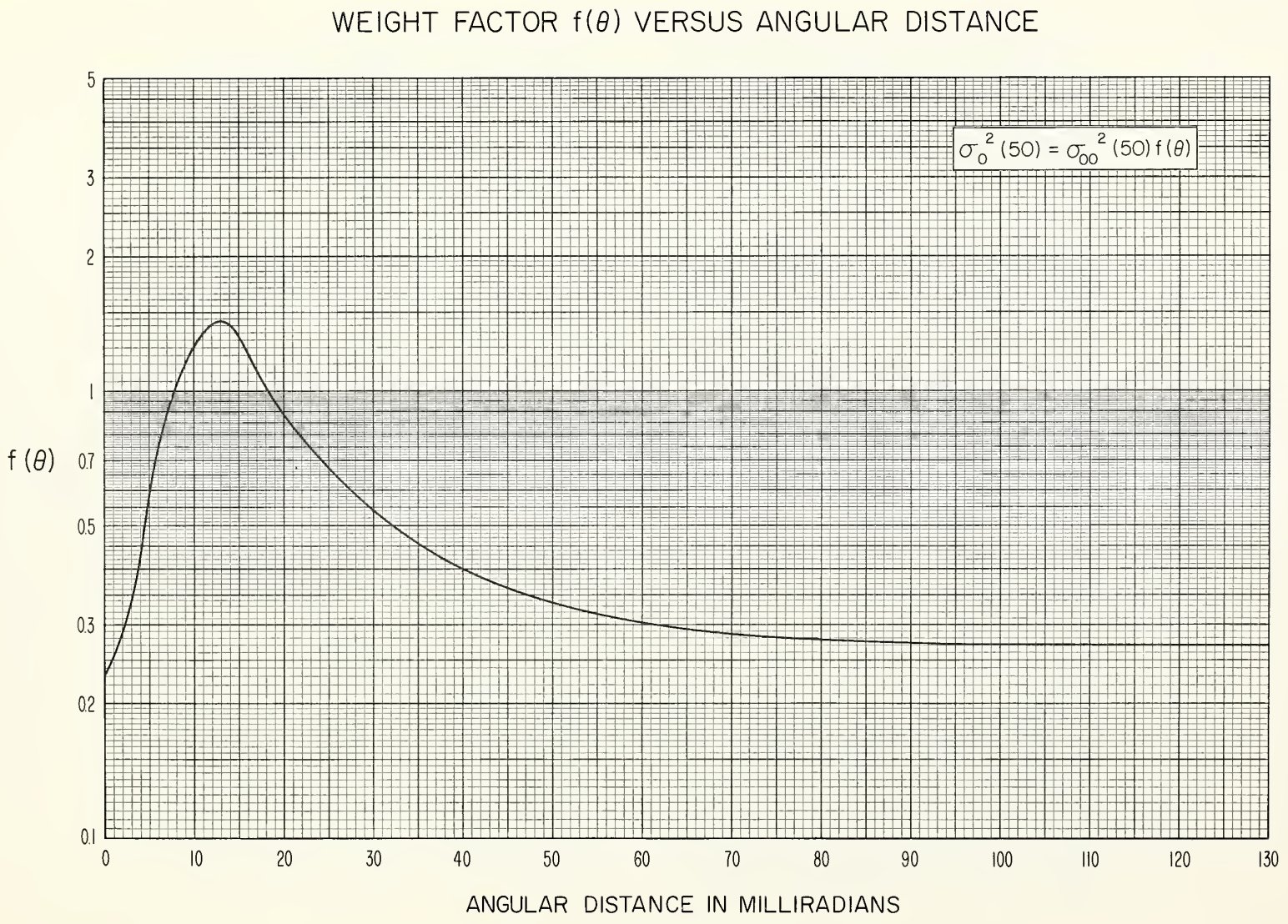
WEIGHT FACTOR f(θ) VERSUS ANGULAR DISTANCE
$\sigma_0^2(50) = \sigma_{00}^2(50) f(\theta)$
f (θ)
5
3
2
1
0.7
0.5
0.3
0.2
0.1
0
10
20
30
40
50
60
70
80
90
100
110
120
130
ANGULAR DISTANCE IN MILLIRADIANS

Figure 6

DISTRIBUTIONS OF HOURLY MEDIANS OF
BASIC TRANSMISSION LOSS ON 1046 MC
FOR SIDI SLIMANE - MORON

Sample Path ($\theta = 40.3$ milliradians)

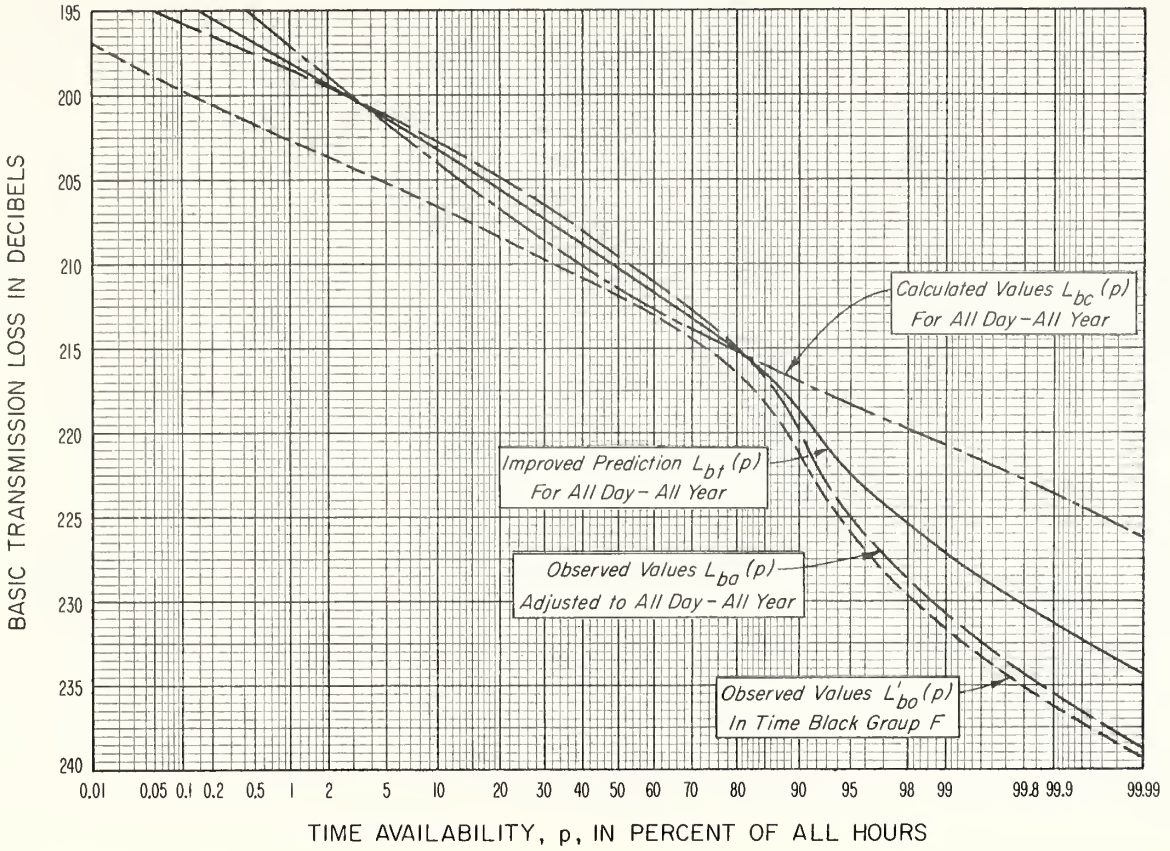

Figure 7

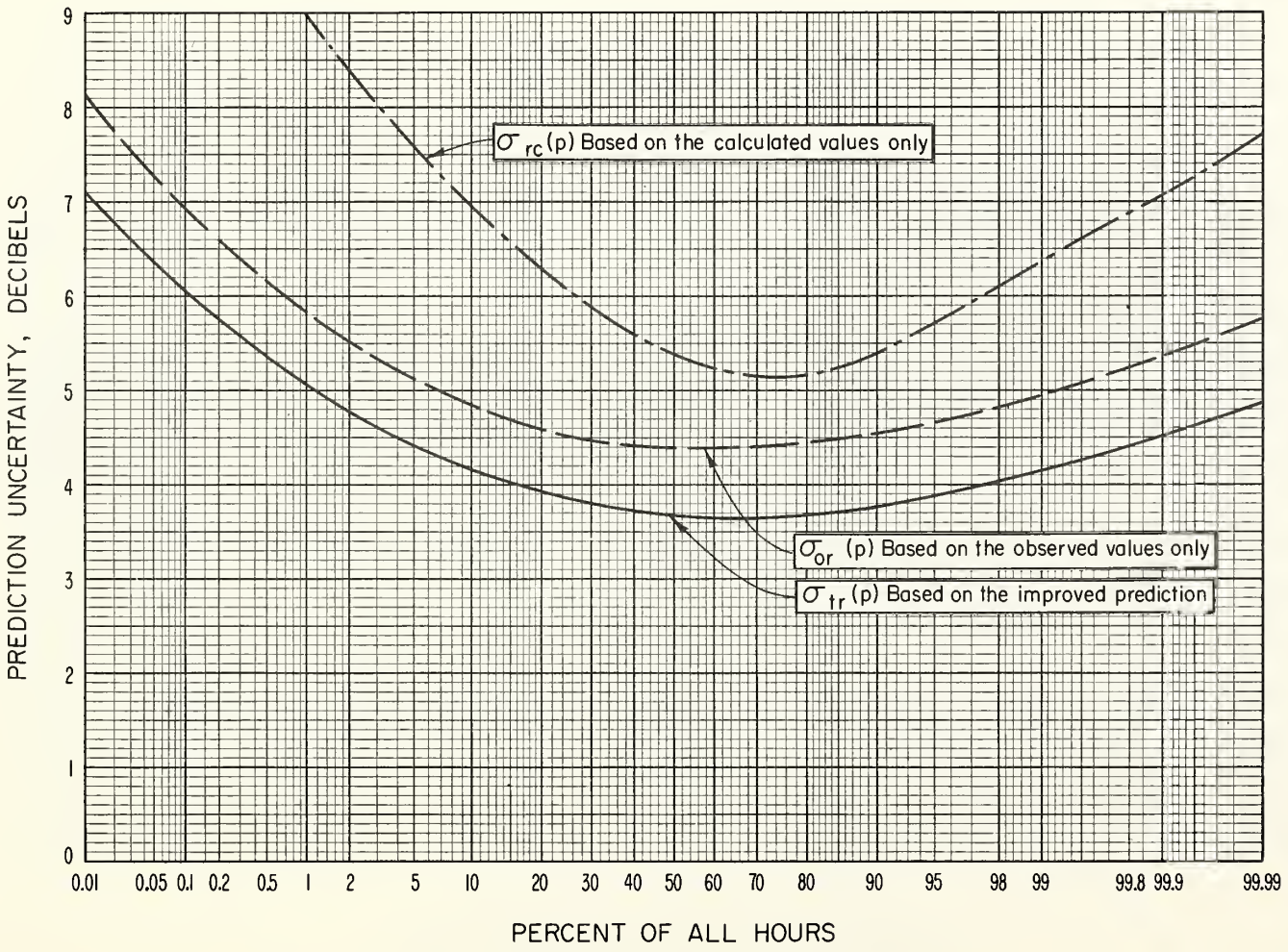
PREDICTION UNCERTAINTY FOR
SIDI SLIMANE - MORON SAMPLE PATH
PREDICTION UNCERTAINTY, DECIBELS
9
8
7
6
5
4
3
2
1
0
σ_{rc} (p) Based on the calculated values only
σ_{or} (p) Based on the observed values only
σ_{tr} (p) Based on the improved prediction
0.01 0.05 0.1 0.2 0.5 1 2 5 10 20 30 40 50 60 70 80 90 95 98 99 99.8 99.9 99.99
PERCENT OF ALL HOURS

Figure 8

SERVICE PROBABILITIES FOR QUADRUPLE DIVERSITY FM SYSTEM, SIDI SLIMANE TO MORON

Sample Path, 850 Mc, 60 Ft. Dishes, 24 Voice Channels, Less Than 1 in 10,000 Character Errors on Teletype

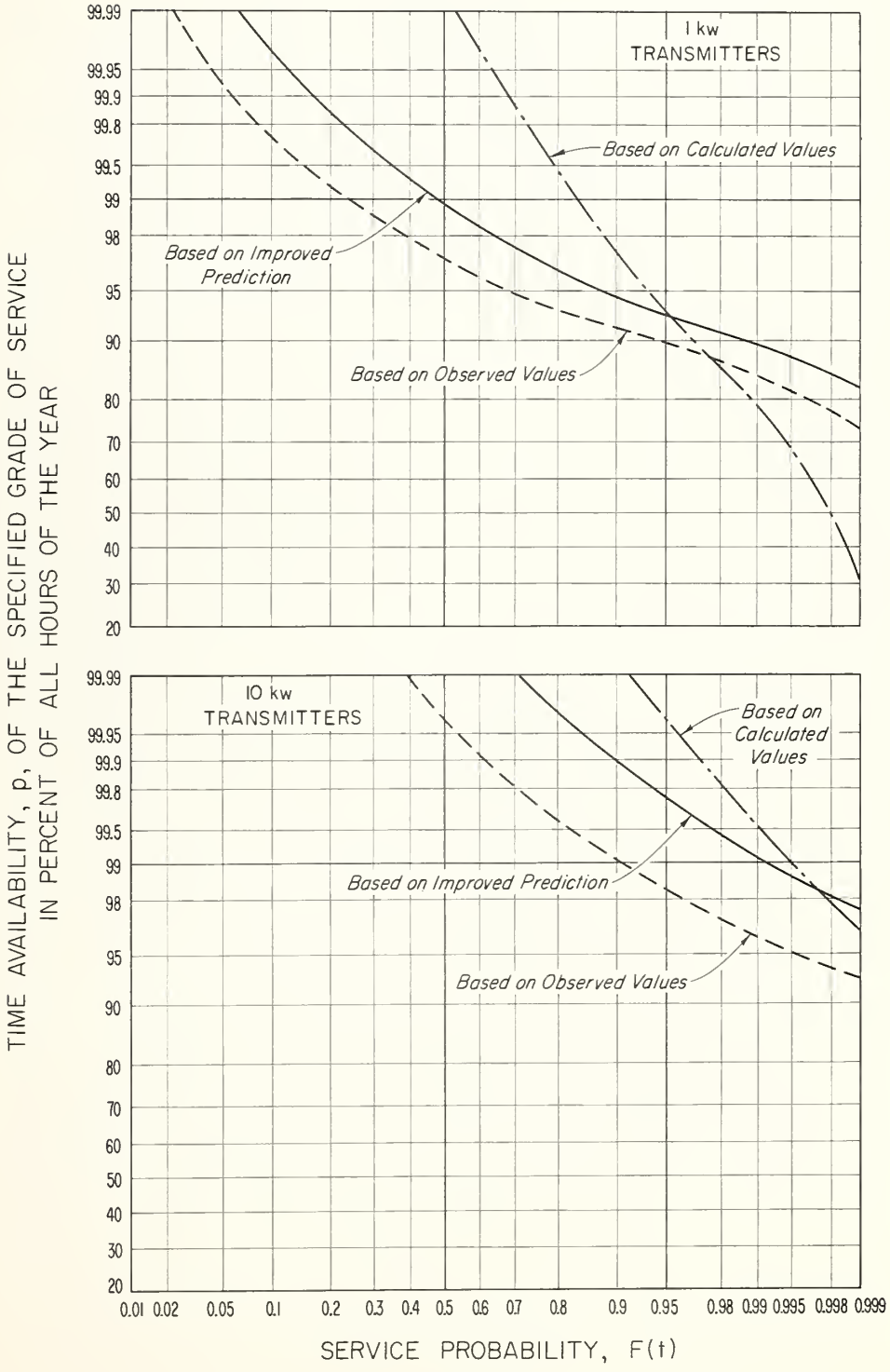

Figure 9

MEASURED DISTRIBUTIONS OF HOURLY MEDIAN BASIC TRANSMISSION LOSS VALUES

KXOK - FM to Urbana Path, 93.7 Mc

d = 146.5 Miles, θ = 19.3 Milliradians

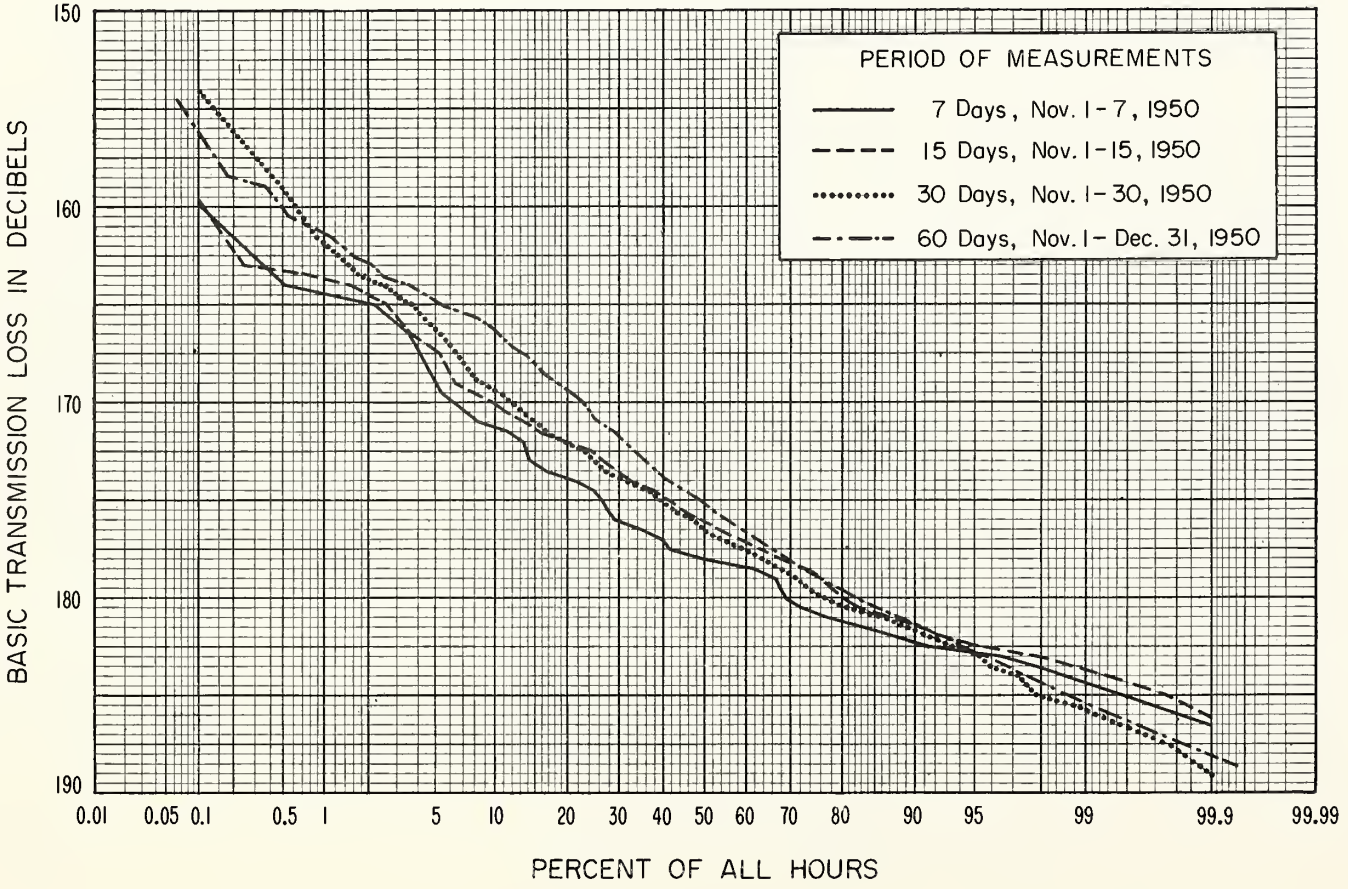

Figure 10

CALCULATED AND MEASURED DISTRIBUTIONS OF
HOURLY MEDIAN BASIC TRANSMISSION LOSS VALUES

KXOK - FM to Urbana Path, 93.7 Mc

d = 146.5 Miles, θ = 19.3 Milliradians

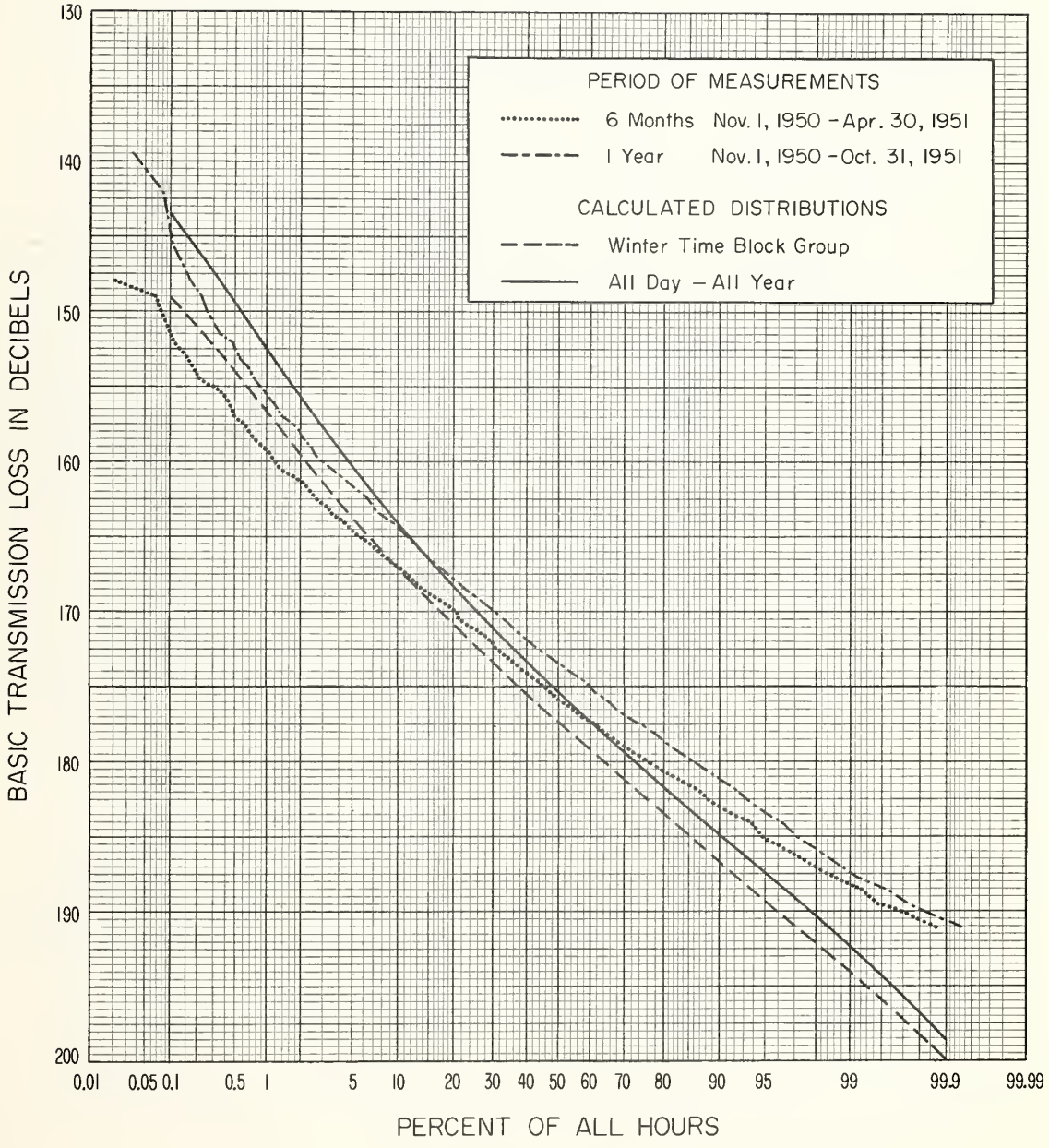

Figure 11

DISTRIBUTIONS OF HOURLY MEDIANS OF BASIC TRANSMISSION LOSS FOR KXOK - FM TO URBANA PATH

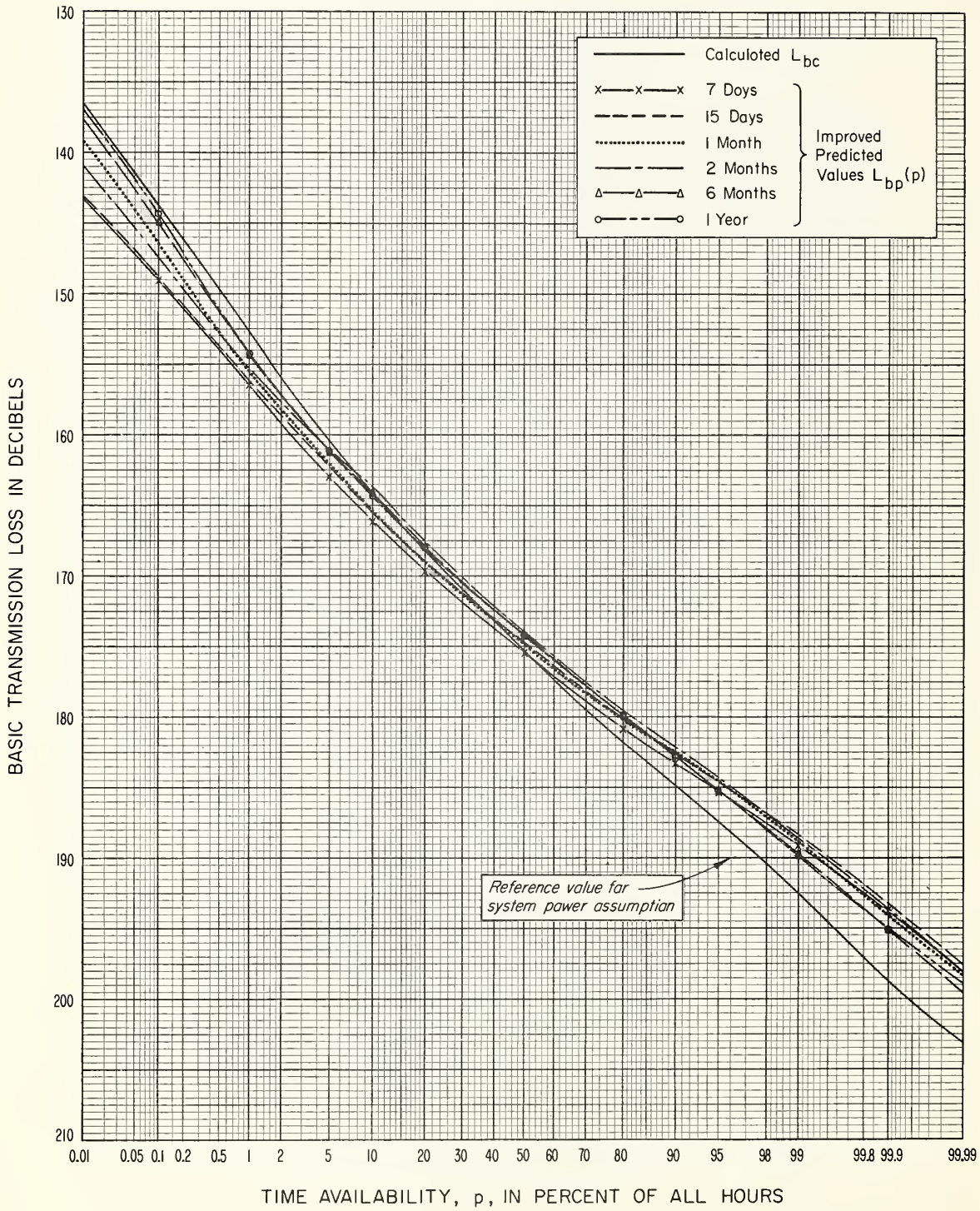

Figure 12

PREDICTION UNCERTAINTY FOR KXOK - FM TO URBANA PATH

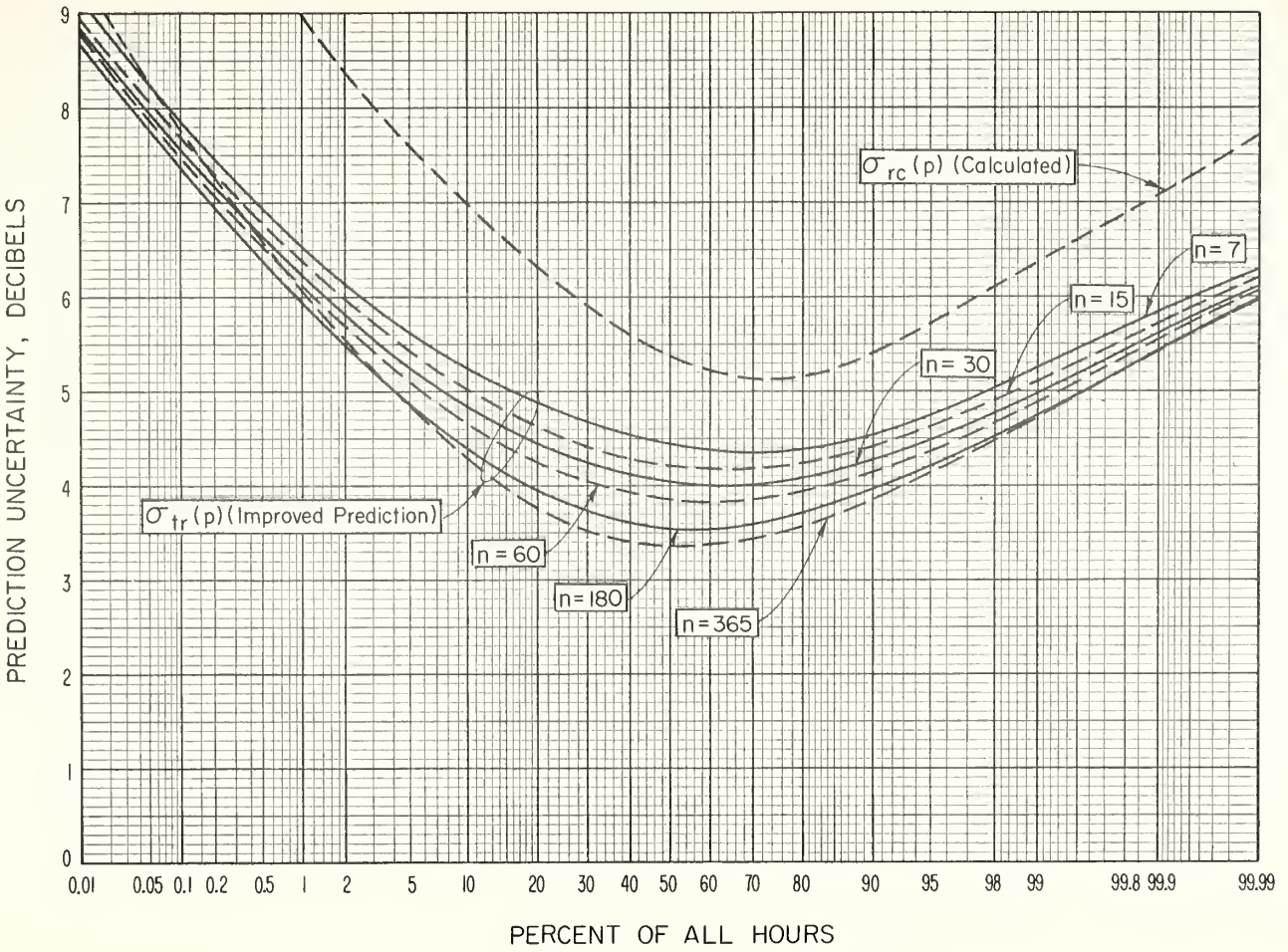

Figure 13

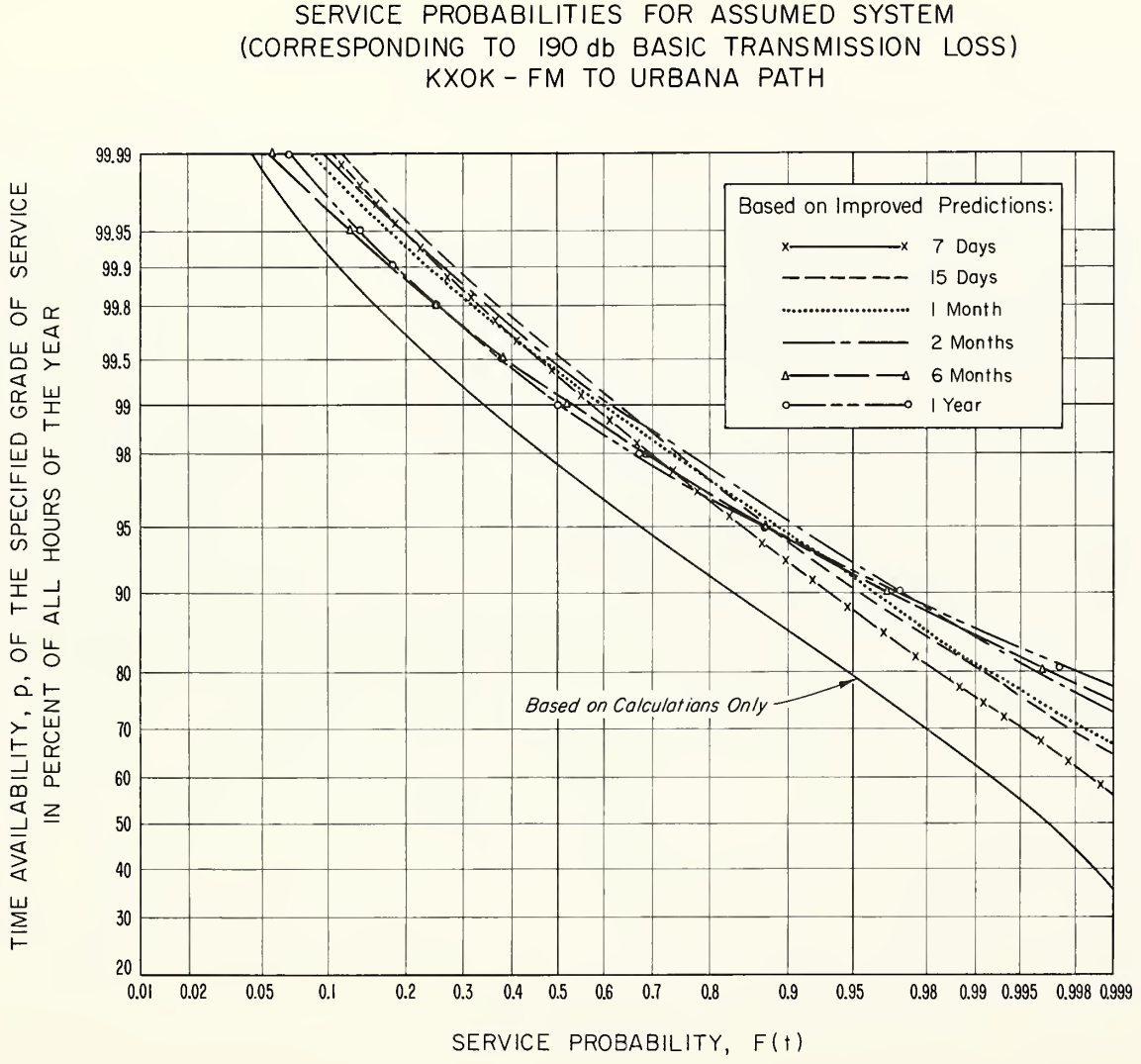
SERVICE PROBABILITIES FOR ASSUMED SYSTEM
(CORRESPONDING TO 190 db BASIC TRANSMISSION LOSS)
KXOK - FM TO URBANA PATH
TIME AVAILABILITY, p, OF THE SPECIFIED GRADE OF SERVICE
IN PERCENT OF ALL HOURS OF THE YEAR
99.99
99.95
99.9
99.8
99.5
99
98
95
90
80
70
60
50
40
30
20
0.01
0.02
0.05
0.1
0.2
0.3
0.4
0.5
0.6
0.7
0.8
0.9
0.95
0.98
0.99
0.995
0.998
0.999
SERVICE PROBABILITY, F(t)
Based on Improved Predictions:
7 Days
15 Days
1 Month
2 Months
6 Months
1 Year
Based on Calculations Only

Figure 14

LENGTH OF MEASUREMENT PERIOD NECESSARY TO RESULT IN
EQUAL PREDICTION UNCERTAINTY FOR CALCULATED AND OBSERVED VALUES

The Curves Are Labelled With the Time Availability, p, in Percent of All Hours

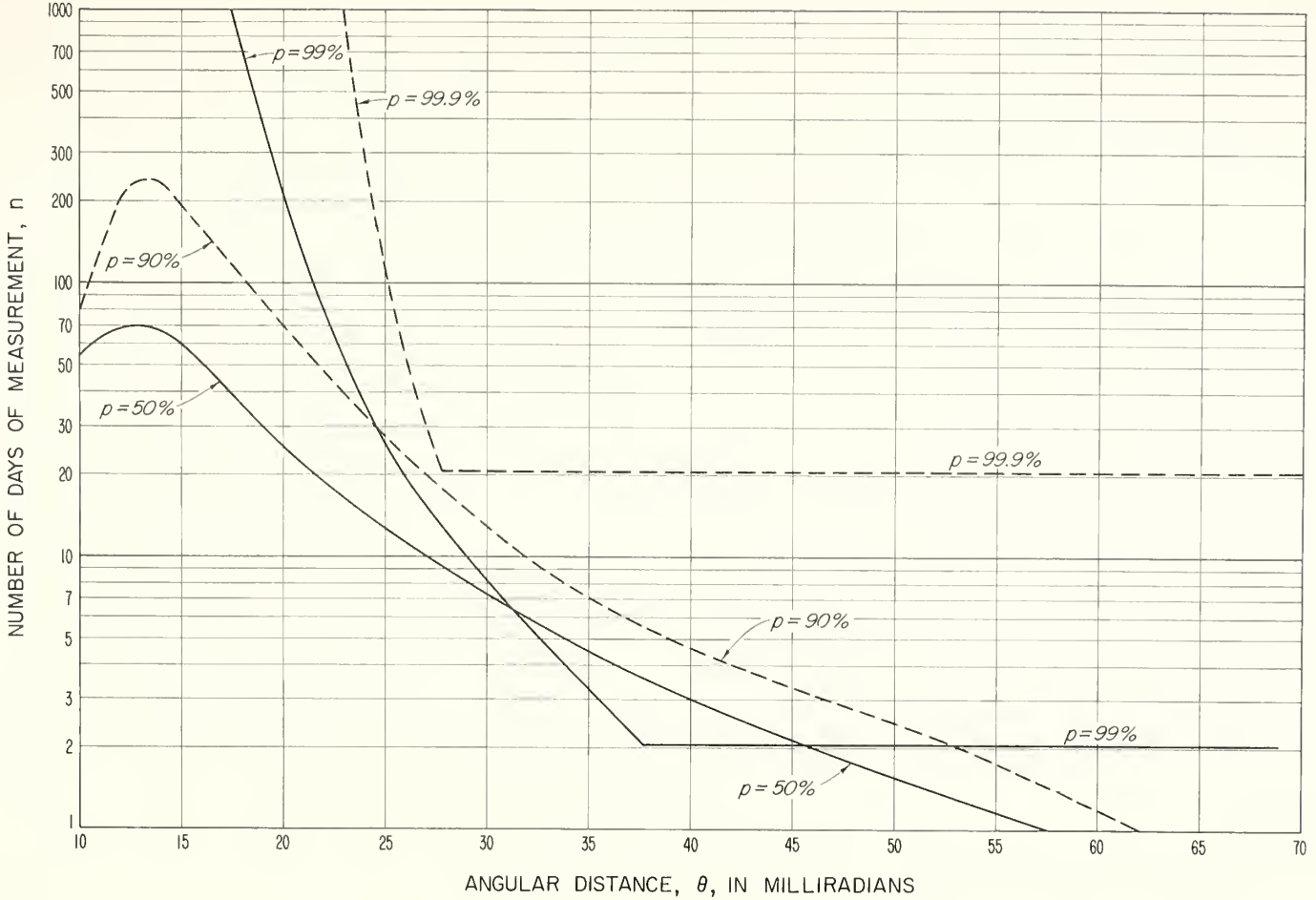

Figure 15

APPENDIX I

Definitions of Terms

This table contains most of the symbols and terms used in Secs. 2, 3, and 4 of this paper.

$L_{bc}(p)$ - calculated hourly median basic transmission loss not exceeded* during at least p% of all hours within the time block, or the time block combinations considered. If desired, p may have a subscript denoting the number of the time block, and subscripts F and S may be used to denote combined Time Blocks 1, 2, 3, 8 (all hours, winter, and 4, 5, 6, 7 (all hours, summer), respectively. Thus, L_{bm} from Sec. 3 of Ref. 1 may be designated $L_{bc}(50_2)$. For the definition of the time blocks, see p. 11.

$\sigma_c(p)$ - standard deviation characterizing the prediction uncertainty of a calculated value $L_{bc}(p)$

$w_c(p) = \frac{1}{\sigma_c^2(p)}$ - weight assigned to the calculated value $L_{bc}(p)$.

$L_{bo}(p)$ - observed hourly median basic transmission loss value not exceeded during at least p% of all hours

*In terms of field strength, $L_{bc}(p)$ corresponds to the hourly median field strength value exceeded during at least p% of all hours.

within a time period which is defined in the same way as explained for $L_{bc}(p)$ above.

$\sigma_o(p)$ - standard deviation characterizing the uncertainty of any observed value $L_{bo}(p)$ not taking into account errors introduced by the measuring equipment and procedures.

σ_e = standard deviation characterizing errors introduced by measuring equipment and procedures.

$w_o(p) = \frac{1}{\sigma^2_{oe(p)}}$ - weight assigned to the observed value $L_{bo}(p)$, taking into account σ_e:

$$\sigma_{oe}^2(p) = \sigma_o^2(p) + \sigma_e^2$$

σ_r = standard deviation characterizing the uncertainty in estimating the system parameters F (noise figure) and R (median r.m.s. carrier to r.m.s. noise ratio).

$\sigma_{\Delta V}(p) = k(\Delta V)$ - standard deviation associated with the distribution of differences in the long term variable, $V(p, \theta)$; taken for a given value of θ, but for various percentage levels p. The values of $V(p, \theta)$ which define ΔV may be taken in the same, or in different time blocks, or time block groups.

$\sigma_{or}(p)$ - standard deviation characterizing the prediction uncertainty based on measurements only, but including σ_r (see above) in order to be applicable to the evaluation of systems

$$\sigma_{or}^2(p) = \sigma_{oe}^2(p) + \sigma_r^2$$

$L_{bt}(p)$ - weighted average of predicted and observed transmission loss values $L_{bc}(p)$ and $L_{bo}(p)$ (see above).

$\sigma_t(p)$ - standard deviation characterizing the remaining prediction uncertainty associated with the weighted average $L_{bt}(p)$

$$\frac{1}{\sigma_t^2(p)} = w_t(p) = w_o(p) + w_c(p)$$

$\sigma_{tr}^2(p)$ - standard deviation characterizing the remaining prediction uncertainty of $L_{bt}(p)$ as based on both prediction and measurements, and including σ_r (see above) in order to be applicable to the evaluation of systems

$$\sigma_{tr}^2(p) = \sigma_t^2(p) + \sigma_r^2$$

APPENDIX II

Estimating the Prediction Uncertainty on the Basis of Measurements Over a Different Path

Starting from (2) in Sec. 2 of the report:

$$L_{tb} = L_{ta} + (L_{cb} - L_{ca}) \qquad \text{(II-1)}$$

This means that the improved prediction for Path b may be expressed as the improved prediction for Path a plus the difference in the calculated values for the two paths. The improved prediction L_{ta} for Path a was given by (1) of Sec. 2:

$$L_{ta} = \frac{w_{oa} L_{oa} + w_{ca} L_{ca}}{w_o + w_{ca}} \qquad \text{(II-2)}$$

Its uncertainty may be expressed by the variance σ_{ta}^2, which is the reciprocal of the sum of the weights $w_{oa} + w_{ca}$ (denominator of II-2).

The predicted values L_{ca} and L_{cb} include the true values L_a and L_b plus the prediction errors ϵ_a and ϵ_b:

$$L_{ca} = L_a + \epsilon_a; \; L_{cb} = L_b + \epsilon_b \qquad \text{(II-3)}$$

The observed value L_{oa} appearing in (II-2) is the sum of the true value L_a and a measurement error δ_a

$$L_{oa} = L_a + \delta_a \qquad \text{(II-4)}$$

The true values L_a and L_b are constants, and the errors δ_a, ϵ_a, and ϵ_b are statistical variables with means of zero for each, and their variances given by $\sigma_{oa}^2 = 1/w_{oa}$, $\sigma_{ca}^2 = 1/w_{ca}$, and $\sigma_{cb}^2 = 1/w_{cb}$, respectively.

Inasmuch as the expected values of L_{ta} and L_{tb}, as well as L_{ca} and L_{cb}, are L_a and L_b, (II-1) reduces to the identity

$$L_b - L_a = L_b - L_a \qquad \text{(II-5)}$$

when written in terms of expected values.

The variance of the linear combination of the three terms in (II-1) is given by[1/]

$$\sigma_{tb}^2 = \sigma_{ta}^2 + \sigma_{ca}^2 + \sigma_{cb}^2 - 2\sigma_{ta}\,\sigma_{ca}\,\rho_{12} + 2\sigma_{ta}\,\sigma_{cb}\,\rho_{13}$$

$$- 2\sigma_{ca}\,\sigma_{cb}\,\rho_{23} \qquad \text{(II-6)}$$

In (II-6) above ρ_{12} designates the correlation coefficient between the improved prediction L_{ta} and the calculated value L_{ca} for Path a, ρ_{13} the correlation coefficient between the improved prediction L_{ta} for Path a and the calculated value L_{cb} for Path b, and ρ_{23} the correlation coefficient between the calculated value L_{ca} for Path a, and the cal-

---

1/ See, for instance, C. A. Bennett and N. L. Franklin, "Statistical analysis in chemistry and the chemical industry," John Wiley and Sons, Inc., New York, 1954. See p. 50.

culated value L_{cb} over Path b.

From Ref. 1 (see p. 37) the correlation coefficient ρ_{xy} between the variables x and y may be written as

$$\rho_{xy} = \frac{E(xy) - E(x)\,E(y)}{\sigma_x\,\sigma_y} \qquad \text{(II-7)}$$

where E(x), E(y), and E(xy) denote here expected values of the variables x, y, and of their product xy.

Thus,

$$\rho_{12} = \frac{E(L_{ta}L_{ca}) - E(L_{ta})\,E(L_{ca})}{\sigma_{ta}\,\sigma_{ca}} \qquad \text{(II-8)}$$

Substituting (II-2) and (II-3) into (II-8), and noting that

$$\frac{1}{w_{oa} + w_{oc}} = \sigma_{ta}^2, \text{ we obtain}$$

$$\rho_{12} = \frac{1}{\sigma_{ta}\,\sigma_{ca}} \left\{ E\left[\sigma_{ta}^2 \left(w_{oa} L_{oa} L_{ca} + w_{ca} L_{ca}^2\right) \right] \right.$$

$$- E\left[\sigma_{ta}^2 \left(w_{oa} L_{oa} + w_{ca} L_{ca}\right) \right]$$

$$\left. - E\left[\sigma_{ta}^2 \left(w_{oa} L_{oa} + w_{ca} L_{ca}\right) \right] \cdot E\left[L_{ca} \right] \right\} \qquad \text{(II-9)}$$

Expanding the various terms separately,

$$E\left[L_{oa}\,L_{ca}\right] = E\left[(L_a - \delta_a)(L_a - \epsilon_a)\right]$$

$$= E\left[L_a^2 - \delta_a L_a - \epsilon_a L_a + \delta_a \epsilon_a\right] = L_a^2, \qquad \text{(II-10)}$$

As $E(\delta_a \epsilon_a)$ equals zero for the reasonable assumption that the prediction and measurement errors are not correlated,

$$E\left[L_{ca}^2\right] = E\left[L_a^2 - 2L_a \epsilon_a + \epsilon_a^2\right] = L_a^2 + \sigma_{ca}^2 \qquad \text{(II-11)}$$

$$E\left[\sigma_{ta}^2(w_{oa} L_{oa} + w_{ca} L_{ca})\right] \cdot E\left[L_{ca}\right] = L_a^2 \qquad \text{(II-12)}$$

Finally,

$$\rho_{12} = \frac{1}{\sigma_{ta}\,\sigma_{ca}} \left\{\sigma_{ta}^2\left[w_{oa} L_a^2 + w_{ca}(L_a^2 + \sigma_{ca}^2)\right] - L_a^2\right\}$$

$$= \frac{1}{\sigma_{ta}\,\sigma_{ca}} \left\{\sigma_{ta}^2(w_{oa} + w_{ca})\, L_a^2 + \sigma_{ta}^2 - L_a^2\right\} = \frac{\sigma_{ta}}{\sigma_{ca}} \qquad \text{(II-13)}$$

Similarly,

$$\rho_{13} = \frac{E(L_{ta}\,L_{cb}) - E(L_{ta}) \cdot E(L_{cb})}{\sigma_{ta}\,\sigma_{cb}} \qquad \text{(II-14)}$$

$$\rho_{13} = \frac{1}{\sigma_{ta}\,\sigma_{cb}} \left\{ E\left[\sigma_{ta}^2 (w_{oa} L_{oa} L_{cb} + w_{ca} L_{ca} L_{cb})\right] \right.$$

$$\left. - E\left[\sigma_{ta}^2 (w_{oa} L_{oa} + w_{ca} L_{ca})\right] \cdot E\left[L_{cb}\right] \right\} \qquad \text{(II-15)}$$

Analogous to (II-10),

$$E\left[L_{oa} L_{cb}\right] = E\left[(L_a - \delta_a)(L_b - \epsilon_b)\right] = L_a L_b, \qquad \text{(II-16)}$$

and

$$E\left[L_{ca} L_{cb}\right] = E\left[(L_a - \epsilon_a)(L_b - \epsilon_b)\right]$$

$$= L_a L_b + \sigma_{ca}\,\sigma_{cb}\,\rho_{ab} \qquad \text{(II-17)}$$

from (II-7), where ρ_{ab} is the correlation coefficient between the calculated values L_{ca} and L_{cb} for Paths a and b, respectively. Then,

$$\rho_{13} = \frac{1}{\sigma_{ta}\,\sigma_{cb}} \left\{ \sigma_{ta}^2 w_{oa} L_a L_b + \sigma_{ta}^2 w_{ca} L_a L_b \right.$$

$$+ \sigma_{ta}^2 w_{ca}\,\sigma_{ca}\,\sigma_{cb}\,\rho_{ab} - \sigma_{ta}^2 w_{oa} L_a L_b$$

$$\left. - \sigma_{ta}^2 w_{ca} L_a L_b \right\} = \frac{\sigma_{ta}}{\sigma_{ca}} \rho_{ab} \qquad \text{(II-18)}$$

ρ_{23} is, of course, identically equal to ρ_{ab}.

Substituting now (II-13), (II-18), and ρ_{ab} into (II-6),

$$\sigma_{tb}^2 = \sigma_{ta}^2 + \sigma_{ca}^2 + \sigma_{cb}^2 - 2\sigma_{ta}\sigma_{ca}\frac{\sigma_{ta}}{\sigma_{ca}}$$

$$+ 2\sigma_{ta}\sigma_{cb}\frac{\sigma_{ta}}{\sigma_{ca}}\rho_{ab} - 2\sigma_{ca}\sigma_{cb}\rho_{ab}$$

$$= \sigma_{ca}^2 + \sigma_{cb}^2 - \sigma_{ta}^2 + 2\sigma_{ca}\sigma_{cb}\rho_{ab}\left(\frac{\sigma_{ta}^2}{\sigma_{ca}^2} - 1\right) \qquad \text{(II-19)}$$

If the two paths, Path a and Path b, are so different that the correlation coefficient between the calculated values may be set equal to zero, (II-19) reduces to

$$\sigma_{tb}^2 = \sigma_{ca}^2 + \sigma_{cb}^2 - \sigma_{ta}^2 \qquad \text{(II-20)}$$

In this case no improvement for Path b is obtained on the basis of measurements for Path a, as σ_{tb}^2 will always be larger than σ_{cb}^2. The latter is the prediction uncertainty of the calculated value for Path b without any measurements, and will in this case be more advantageous to use than σ_{tb}^2. The improved prediction uncertainty σ_{ta}^2 for Path a will, of course, be always smaller than σ_{ca}^2, based only on calculated values, and the right-hand side of (II-20) will always be larger than σ_{cb}^2.

If the Paths a and b are completely identical, $\rho_{ab} = 1$, and

$\sigma_{ca}^2 = \sigma_{cb}^2$. Then (II-19) reduces to the identity

$$\sigma_{tb}^2 = \sigma_{ta}^2 \qquad \text{(II-21)}$$

The case of most interest in practical applications is the one where the paths are nearly equal (i.e., in the same general area of similar meteorological or terrain characteristics, with perhaps one of the terminals identical). In this case the prediction uncertainties σ_{ca}^2 and σ_{cb}^2 are equal[2/].

$$\sigma_{ca}^2 = \sigma_{cb}^2 = \sigma_c^2 \qquad \text{(II-22)}$$

and (II-19) is transformed to

$$\sigma_{tb}^2 = \sigma_{ta}^2(2\rho_{ab} - 1) + 2\sigma_c^2(1 - \rho) \qquad \text{(II-23)}$$

Dividing by σ_c^2, and denoting the prediction improvement ratio for Path b σ_{tb}^2/σ_c^2 as r^2, r^2 may be obtained as a function of the prediction improvement ratio for Path a (for which the measurements are available) $\sigma_{ta}^2/\sigma_c^2 = k^2$, and the correlation coefficient ρ_{ab}:

$$r^2 = k^2(2\rho_{ab} - 1) + 2(1 - \rho_{ab}) \qquad \text{(II-24)}$$

Curves for r^2 have been calculated and are shown on Fig. II-1.

2/ A. P. Barsis, K. A. Norton, and P. L. Rice, "Predicting the performance of long distance communication circuits," NBS Report 6032, December 1958

Only values of $r^2 < 1$ represent an improvement in the prediction for Path b ($\sigma_{tb}^2 < \sigma_c^2$). Fig. II-1 shows that ρ_{ab} has to be at least 0.5, and the improvement for Path b, of course, depends on the degree of improvement $k^2 = \sigma_{ta}^2/\sigma_c^2$ obtained by measurements for Path a. For $k^2 = 1$, ρ_{ab} drops out of (II-24) and $r^2 = 1$ for any value of ρ_{ab}.

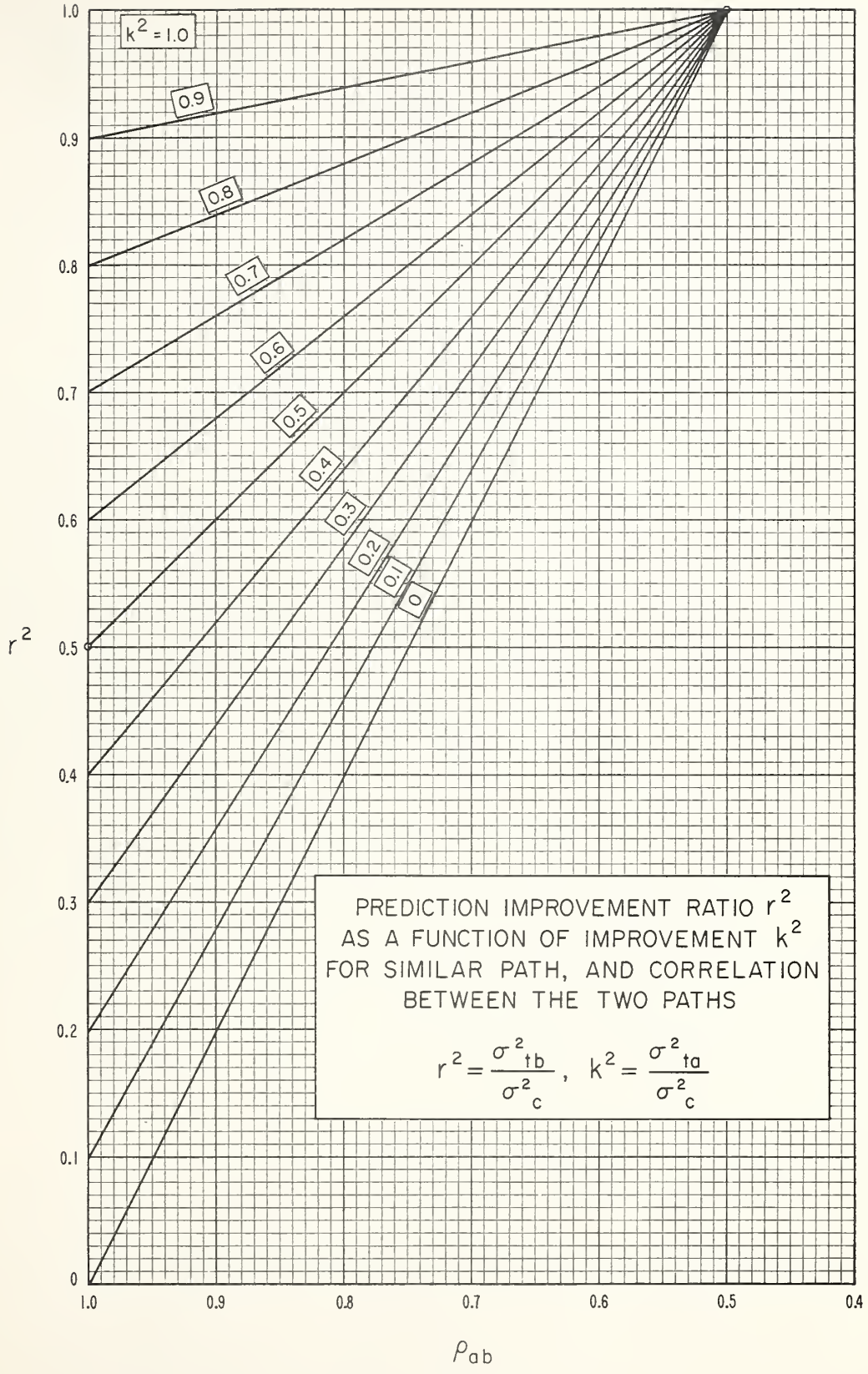
$k^2 = 1.0$
0.9
0.8
0.7
0.6
0.5
0.4
0.3
0.2
0.1
0
r^2
1.0
0.9
0.8
0.7
0.6
0.5
0.4
ρ_{ab}
PREDICTION IMPROVEMENT RATIO r^2
AS A FUNCTION OF IMPROVEMENT k^2
FOR SIMILAR PATH, AND CORRELATION
BETWEEN THE TWO PATHS
$r^2 = \frac{\sigma^2_{tb}}{\sigma^2_c}$, $k^2 = \frac{\sigma^2_{ta}}{\sigma^2_c}$

Figure II - 1

U. S. DEPARTMENT OF COMMERCE
Sinclair Weeks, *Secretary*

NATIONAL BUREAU OF STANDARDS
A. V. Astin, *Director*

THE NATIONAL BUREAU OF STANDARDS

The scope of the scientific program of the National Bureau of Standards at laboratory centers in Washington, D. C., and Boulder, Colorado, is given in the following outline:

Washington, D.C.

Electricity and Electronics. Resistance and Reactance. Electron Devices. Electrical Instruments. Magnetic Measurements. Dielectrics. Engineering Electronics. Electronic Instrumentation. Electrochemistry.

Optics and Metrology. Photometry and Colorimetry. Optical Instruments. Photographic Technology. Length. Engineering Metrology.

Heat. Temperature Physics. Thermodynamics. Cryogenic Physics. Rheology. Engine Fuels. Free Radicals.

Atomic and Radiation Physics. Spectroscopy. Radiometry. Mass Spectrometry. Solid State Physics. Electron Physics. Atomic Physics. Neutron Physics. Nuclear Physics. Radioactivity. X-rays. Betatron. Nucleonic Instrumentation. Radiological Equipment. AEC Radiation Instruments.

Chemistry. Organic Coatings. Surface Chemistry. Organic Chemistry. Analytical Chemistry. Inorganic Chemistry. Electrodeposition. Molecular Structure and Properties. Physical Chemistry. Thermochemistry. Spectrochemistry. Pure Substances.

Mechanics. Sound. Mechanical Instruments. Fluid Mechanics. Engineering Mechanics. Mass and Scale. Capacity, Density, and Fluid Meters. Combustion Controls.

Organic and Fibrous Materials. Rubber. Textiles. Paper. Leather. Testing and Specifications. Polymer Structure. Plastics. Dental Research.

Metallurgy. Thermal Metallurgy. Chemical Metallurgy. Mechanical Metallurgy. Corrosion. Metal Physics.

Mineral Products. Engineering Ceramics. Glass. Refractories. Enameled Metals. Concreting Materials. Constitution and Microstructure.

Building Technology. Structural Engineering. Fire Protection. Air Conditioning, Heating, and Refrigeration. Floor, Roof, and Wall Coverings. Codes and Safety Standards. Heat Transfer.

Applied Mathematics. Numerical Analysis. Computation. Statistical Engineering. Mathematical Physics.

Data Processing Systems. SEAC Engineering Group. Components and Techniques. Digital Circuitry. Digital Systems. Analogue Systems. Application Engineering.

- Office of Basic Instrumentation
- Office of Weights and Measures

Boulder, Colorado
BOULDER LABORATORIES
F. W. Brown, *Director*

Cryogenic Engineering. Cryogenic Equipment. Cryogenic Processes. Properties of Materials. Gas Liquefaction.

Radio Propagation Physics. Upper Atmosphere Research. Ionosphere Research. Regular Propagation Services. Sun-Earth Relationships. VHF Research. Ionospheric Communications Systems.

Radio Propagation Engineering. Data Reduction Instrumentation. Modulation Systems. Navigation Systems. Radio Noise. Tropospheric Measurements. Tropospheric Analysis. Radio Systems Application Engineering.

Radio Standards. High Frequency Electrical Standards. Radio Broadcast Service. High Frequency Impedance Standards. Electronic Calibration Center. Microwave Physics. Microwave Circuit Standards.

Department of Commerce
National Bureau of Standards
Boulder Laboratories
Boulder, Colorado

Official Business

NBS

Postage and Fees Paid
U. S. Department of Commerce